Review

Conducting Polymers in Solar Cells: Insights, Innovations, and Challenges

Aliya Yelshibay [1], Sherif Dei Bukari [1], Bakhytzhan Baptayev [2] and Mannix P. Balanay [1,2,*]

1   Chemistry Department, Nazarbayev University, 53 Kabanbay Batyr Ave., Astana 01000, Kazakhstan; aliya.yelshibay@nu.edu.kz (A.Y.); sherif.bukari@nu.edu.kz (S.D.B.)
2   National Laboratory Astana, Nazarbayev University, 53 Kabanbay Batyr Ave., Astana 010000, Kazakhstan; bbaptayev@nu.edu.kz
*   Correspondence: mannix.balanay@nu.edu.kz

Abstract: The pursuit of sustainable energy sources has led to significant advances in solar cell technology, with conducting polymers (CPs) emerging as key innovations. This review examines how CPs improve the performance and versatility of three important types of solar cells: dye-sensitized solar cells (DSSCs), perovskite solar cells (PSCs), and organic solar cells (OSCs). Polymers such as polyaniline, polypyrrole, and poly(3,4-ethylenedioxythiophene) have shown significant potential to increase the efficiency of solar cells. In DSSCs, conducting polymers act as counter electrodes, electrolytes, and dyes, contributing to improved efficiency and stability. In PSCs, they serve as hole transport materials and electron transport materials that improve charge separation and reduce recombination losses. In OSCs, conducting polymers act as HTMs and active layers, significantly impacting device performance and enabling advances in both binary and ternary solar cell configurations. Recent research highlights the important role of conducting polymers in improving both the efficiency and stability of solar cells under different indoor and outdoor lighting conditions. Recent advances have led to impressive energy conversion efficiencies, particularly in low-light environments. This report also highlights the environmental and economic benefits associated with these materials. At the same time, it highlights the challenges associated with optimizing the materials, scalability, and ensuring long-term stability. Future research directions are outlined to overcome these obstacles and promote the commercial viability of next-generation solar technologies.

Keywords: solar energy; dye-sensitized solar cells; polymer-based counter electrodes; perovskite solar cells; renewable energy; photovoltaics; indoor applications

1. Introduction

Global energy demand has been steadily rising due to population growth and technological progress. From 1990 to 2020, there was a significant 69% increase in global energy consumption, driven largely by the expanding global population [1]. This upward trend is expected to continue in the coming decades. Currently, fossil fuels—coal, oil, and natural gas—dominate the global energy mix, accounting for approximately 81% of total consumption. However, these resources are finite and diminishing rapidly, posing significant challenges to energy security and environmental sustainability. The combustion of fossil fuels also contributes heavily to greenhouse gas emissions, exacerbating climate change and air pollution. In response to these challenges, there is a pressing need to transition towards renewable energy sources such as wind, hydro, geothermal, and biomass. Wind energy, generated by turbines, is a fast-growing renewable source, although its production is variable depending on location and weather conditions [2]. Wind farms can also impact local wildlife, particularly bird and bat populations [3]. Hydropower, another major renewable source, relies on water flow in rivers and dams to generate electricity, but it can cause habitat disruption and community displacement [4]. Geothermal energy harnesses

heat from the Earth's interior, providing a consistent source of power. However, it is viable only in areas with substantial geothermal activity. Nations like Iceland, New Zealand, Kenya, El Salvador, the Philippines, and Costa Rica obtain 12% to 30% of their electricity from geothermal energy [5]. Biomass energy, derived from organic materials, can produce harmful byproducts like fly ash containing heavy metals and hydrocarbons [6]. Among renewables, solar energy emerges as particularly promising due to its abundant availability, sustainability, and minimal environmental impact. Solar radiation has the potential to meet global electricity demands efficiently while reducing pollution [7]. Photovoltaic (PV) technology, utilizing semiconductor materials like silicon, has become pivotal in harnessing solar energy. Solar cells have evolved through three generations: first-generation cells mainly using silicon, second-generation cells incorporating materials like amorphous silicon and thin films, and third-generation cells employing innovative materials such as organic dyes and quantum dots [8–10]. Perovskite solar cells (PSCs) within the third generation have shown significant promise, achieving high efficiencies through simpler, cost-effective fabrication processes compared to traditional silicon cells. However, they face challenges such as device instability, hysteresis, lead toxicity, and color limitations [11,12]. In addition, the perovskite solar cell exhibits reduced stability when exposed to oxygen and humidity, and its complex production process remains a significant barrier to market entry [13]. Organic solar cells (OSCs), on the other hand, offer several advantages. These include their low cost and ability to be prepared at low temperatures, along with mechanical flexibility and compatibility with various substrates. Recent advancements have pushed their energy conversion efficiency to a record 20%, showing potential to surpass traditional silicon cells [14]. However, challenges such as energy production costs and long-term stability still need to be addressed.

Another third-generation solar cell, the dye-sensitized solar cell (DSSC), offers significant advantages over conventional silicon solar cells and other types of third-generation solar cells. DSSCs are particularly easy to manufacture and inexpensive. They can be produced at low temperatures and under non-inert conditions, which is in contrast to the methods commonly used for other types of photovoltaic devices such as PSCs and OSCs. This not only simplifies manufacturing, but also reduces energy consumption during production. In addition to their manufacturing advantages, DSSCs are transparent and flexible, making them ideal for integration into various applications such as building-integrated photovoltaics and portable electronics. Their environmental friendliness also extends to indoor and window modules, further expanding their practical applications [15,16]. Dye-sensitized solar cells thus represent a promising alternative in the field of solar technology, characterized by versatility and sustainability in various applications and environments.

Efficiency comparisons among different solar cell generations are illustrated in Figure 1. First-generation solar cells such as crystalline silicon (c-Si), Si double-sided wafer cells (DS wafer cells), and Si thin transfer submodule cells achieve power conversion efficiency (PCE) of 26.8%, 24.4%, and 21.2%, respectively. In contrast, second-generation photovoltaics like CIGS, CdTe, and amorphous Si exhibit lower efficiencies at 23.4%, 21.0%, and 10.2%, respectively [17]. Moving to third-generation solar cells, a diverse range of efficiency values is observed. Perovskite cells stand out with an impressive 28.8% efficiency in tandem configuration [18] and 26.1% in single-junction configuration [19]. Dye-sensitized solar cells achieve a more modest 15.2% efficiency [20], while binary organic solar cells reach 19.7% PCE [14]. Indoors, DSSCs demonstrate competitive efficiency at 36.3% [21], similar to OSCs at 36.3% [22] and triplet-cation PSCs at 40.2% [23] under 1000 lux irradiation. Continued research and development efforts are essential to fully exploit the potential of these technologies for widespread adoption in the solar energy market. This review paper focuses on dye-sensitized, perovskite, and organic solar cells as representatives of third-generation photovoltaics, offering a comprehensive overview of their current status and future prospects, with a particular emphasis on the pivotal role of conducting polymers.
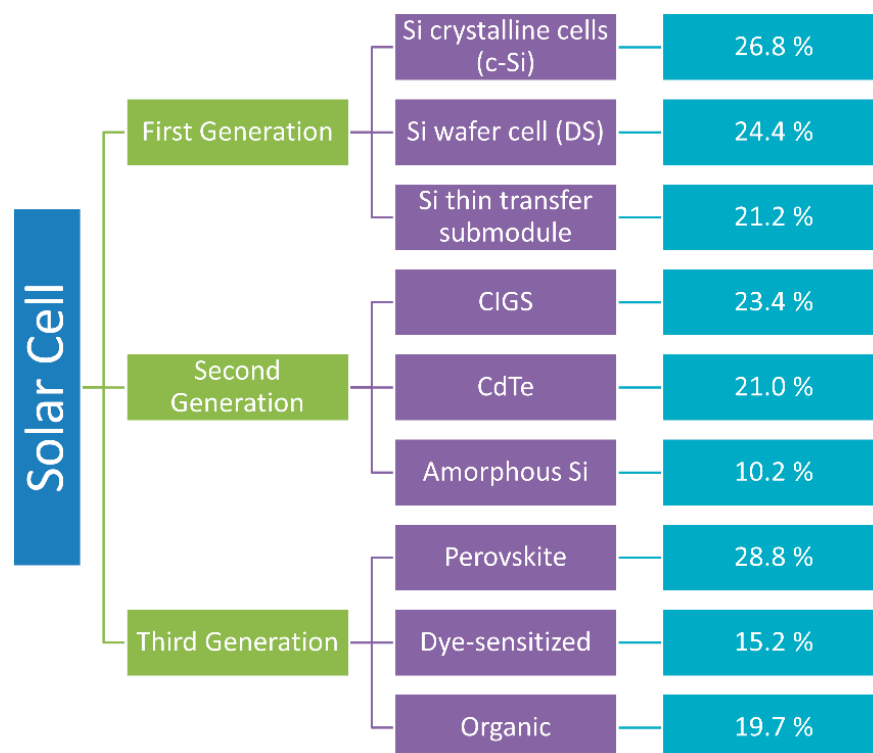
Figure 1. Comparison of power conversion efficiencies across different generations and types of solar cells. Data for first- and second-generation solar cells are sourced from [17], while the PCE values for perovskite, dye-sensitized, and organic solar cells are obtained from references [14,18,20], respectively.

2. Fundamentals of Solar Cells

2.1. Perovskite Solar Cells

Perovskite solar cells represent a promising advancement in photovoltaic technology, achieving high power conversion efficiencies rapidly [24]. These cells utilize organometal halide light absorbers known for their superior optical absorption and balanced charge transport properties. Contrary to previous assumptions of a p-i-n structure, the working principle involves the formation of a p-n junction. Perovskite materials exhibit advantageous characteristics such as long carrier diffusion lengths, low exciton binding energies, and intrinsic ferroelectric properties [25,26]. Illustrated in Figure 2, a typical perovskite solar cell comprises FTO/ITO-coated glass, a hole-blocking layer, an electron-transporting layer, perovskite, a hole-transporting layer, and a metallic counter electrode. When sunlight strikes the perovskite layer, it energizes electrons from the valence band (HOMO) to the conduction band (LUMO), leaving holes behind. These excited electrons migrate to the electron transport layer or material (ETL or ETM) and diffuse towards the front contact, while holes move through the hole transport layer or material (HTL or HTM). The HTM facilitates hole passage to the external circuit and impedes electron flow. Efficient charge separation and transport occur at the interfaces of these layers. For optimal power generation, the perovskite layer ideally features a bandgap of 1.1–1.4 eV to effectively absorb visible light. The conduction band of the perovskite should marginally exceed that of the ETM for efficient electron transfer, while the valence band should slightly trail that of the HTM for effective hole transfer [27–29].
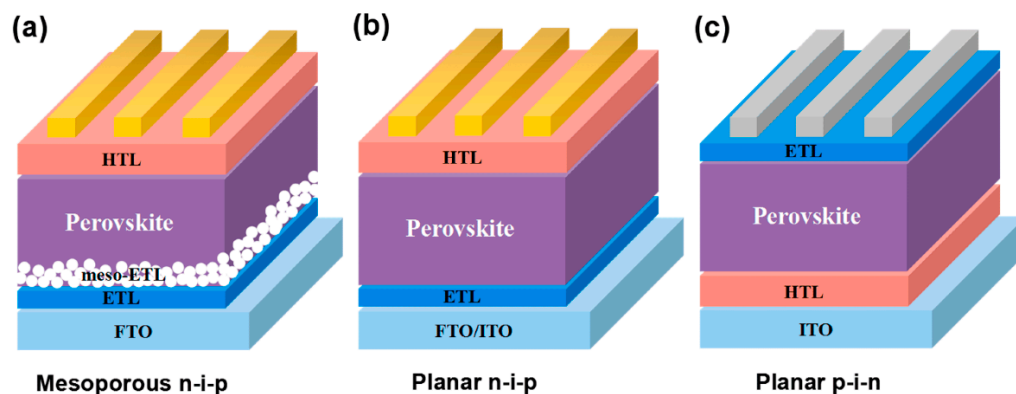
Figure 2. Various configurations of perovskite solar cells. (**a**) Mesoporous structure, (**b**) standard n-i-p configuration, and (**c**) p-i-n configuration. Adapted with permission from reference [30]. Copyright (2022) the authors, some rights reserved; exclusive licensee MDPI. Distributed under a Creative Commons Attribution 4.0 International License (CC BY 4.0).

2.2. Dye-Sensitized Solar Cells

Dye-sensitized solar cells comprise three main components: the dye sensitized photoanode, electrolyte, and counter electrode, each crucial for the cell's efficiency and performance. The photoanode, typically composed of dye-sensitized nanocrystalline titanium dioxide (TiO_2), plays a dual role in light absorption and charge carrier transport, with its thickness directly influencing cell performance [31,32]. The electrolyte, whether liquid or solid, facilitates charge transfer and dye regeneration, for instance, liquid electrolytes like the I^-/I_3^- redox couple. The counter electrode (CE) optimizes cell performance by facilitating charge transport, preventing recombination losses, and ensuring long-term durability [33]. Therefore, selecting appropriate CE materials and designs is crucial for maximizing overall performance and reliability of solar cell devices. Understanding the operational principles of DSSCs is essential (Figure 3). When sunlight strikes the DSSC, photons are absorbed by light-sensitive dye molecules. These dyes typically contain chromophores capable of capturing photons across a wide spectrum. Upon absorption, the dye molecule becomes excited, promoting an electron to a higher energy state and creating an electron–hole pair. The excited electron is then injected from the dye molecule into the conduction band of a semiconductor material, such as TiO_2, which acts as an electron acceptor. These injected electrons flow through the semiconductor material towards the conductive substrate, often a transparent conductive oxide (TCO) like fluorine-doped tin oxide (FTO), generating an electric current. Simultaneously, the dye molecule, now electron-deficient, undergoes a redox reaction with the electrolyte present in the cell, regenerating the dye by accepting an electron from the electrolyte, which acts as an electron donor. The electrons collected at the conductive substrate flow through an external circuit, powering electrical devices before returning to the dye molecule through the counter electrode. At the counter electrode, usually catalyzed with materials like platinum, these electrons are transferred to the electrolyte, completing the redox reaction and regenerating the electrolyte for subsequent cycles [34–38].

2.3. Organic Solar Cells

Organic solar cells utilize organic materials to convert sunlight into electricity. Typically, these materials include conjugated polymers and small organic molecules. A typical organic solar cell structure consists of a photoactive layer positioned between two electrodes. This layer comprises a blend of electron-donor and electron-acceptor materials. For instance, common donor materials are conjugated polymers such as poly(3-hexylthiophene) (P3HT), while acceptors often include fullerene derivatives like [6]-phenyl-C61-butyric acid methyl ester ($PC_{61}BM$) [39].
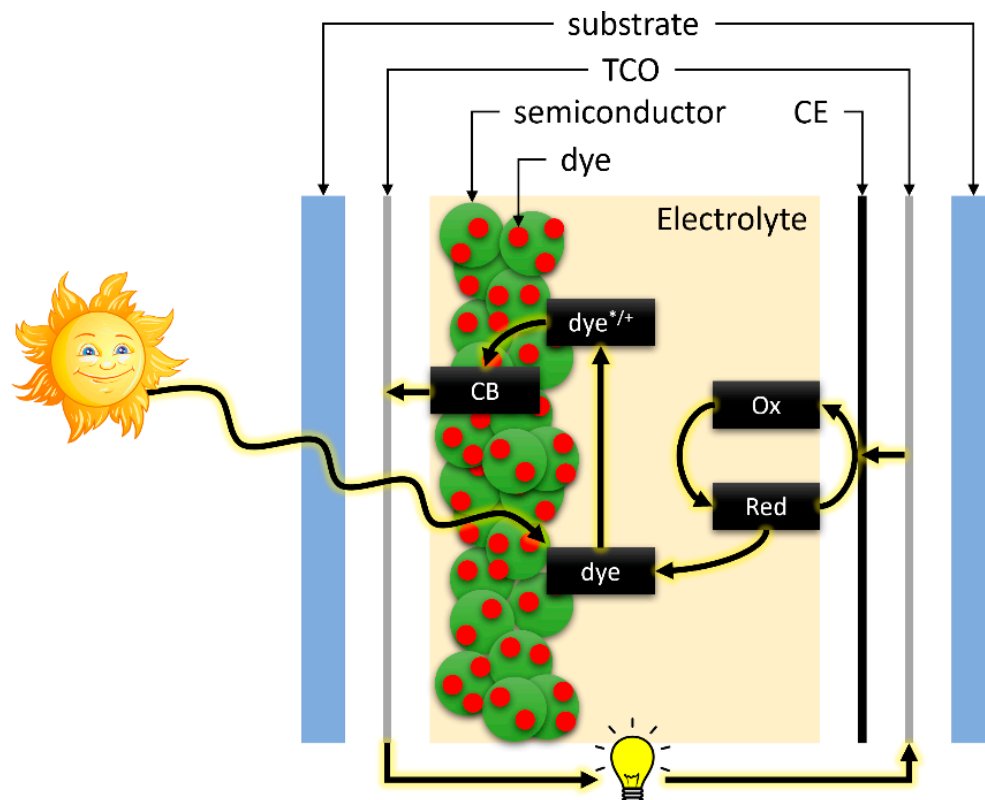
Figure 3. Working principle of dye-sensitized solar cells. Adapted with permission [38], copyright (2022) Springer Nature.

Organic solar cells generally consist of multiple layers (Figure 4): an initial electrode, an electron transport layer, the photoactive layer, a hole transport layer, and a final electrode. The operation of these cells begins with the absorption of light, which generates electron–hole pairs (excitons). These excitons then migrate to the interface between the donor and acceptor materials, where they dissociate into free electrons and holes. Electrons flow through the acceptor material to the cathode, while holes move through the donor material to the anode, thus producing an electric current that can power devices [40,41]. Despite typically having lower power conversion efficiency compared to their inorganic counterparts, organic solar cells offer advantages such as lower cost and flexibility.

2.4. Efficiency of Solar Cells

To fully comprehend the efficiency of solar cells, it is essential to explore the key parameters that govern their performance. The primary measure of efficiency is power conversion efficiency, which quantifies how effectively a solar cell transforms incident sunlight into electrical power. This efficiency is calculated using the formula

$$\text{PCE} = \frac{J_{SC} \times V_{OC} \times FF}{I_{in}} \tag{1}$$

where J_{SC} denotes the short-circuit current density, V_{OC} is the open-circuit voltage, FF stands for the fill factor, and I_{in} is the incident light intensity. Each of these factors plays a pivotal role in determining the overall performance of the solar cell.

The short-circuit current density is a crucial parameter representing the maximum current a solar cell can produce when its terminals are shorted, meaning no external voltage is applied. J_{SC} indicates the cell's capability to generate current under standard illumination conditions. Higher J_{SC} values generally correlate with a greater potential for power output, provided other factors such as voltage and fill factor are also optimized. The

effectiveness of J_{SC} is influenced by factors like light absorption, material properties, and surface recombination losses.
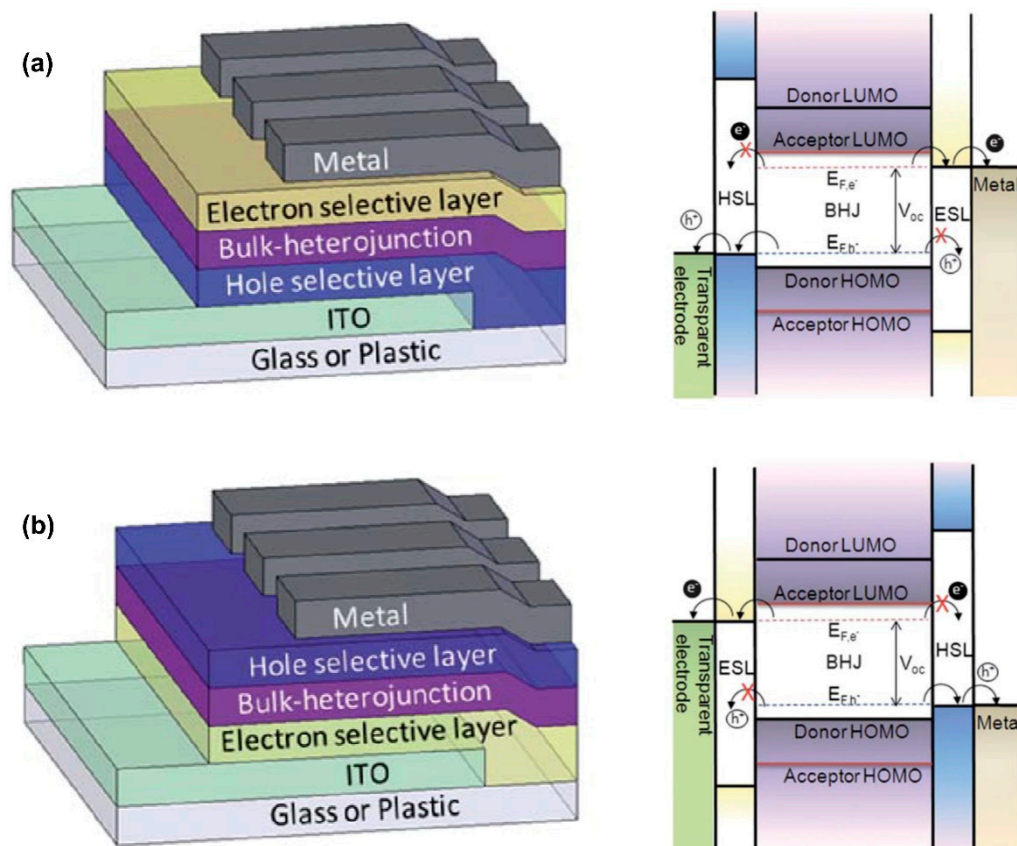
Figure 4. Working principle of organic solar cell with (**a**) conventional and (**b**) inverted configurations. Adapted with permission [42], copyright (2012) Royal Society of Chemistry.

In contrast, the open-circuit voltage signifies the maximum voltage a solar cell can produce when no current flows, thus reflecting the voltage potential under no-load conditions. This parameter is a critical determinant of the cell's voltage-generating capability. The V_{OC} value is influenced by factors such as the semiconductor material's bandgap, temperature variations, and the intensity of incident light. A higher V_{OC} indicates a greater potential voltage output, contributing to improved efficiency.

The fill factor assesses the solar cell's effectiveness in utilizing the current–voltage (I-V) curve to produce power. It is defined as the ratio of the maximum power output to the product of V_{OC} and J_{SC}. A higher *FF* indicates that the solar cell can convert a greater proportion of the theoretical maximum current and voltage into actual power. FF is influenced by series resistance, shunt resistance, and the overall shape of the I-V curve, with higher values reflecting better efficiency and quality of the cell.

Lastly, the incident light intensity or solar irradiance measures the amount of solar energy per unit area incident on the solar cell. Typically expressed in watts per square meter (W/m^2) or in terms of "suns" (where 1 sun equals 1000 W/m^2), I_{in} directly affects the amount of power a solar cell can generate. Variations in I_{in} are due to factors such as the time of day, weather conditions, and geographical location. Higher light intensity leads to greater energy availability for conversion, thereby impacting the solar cell's efficiency.

Thus, understanding and optimizing these parameters are crucial for evaluating and enhancing the performance of solar cells. Each parameter contributes to the overall efficiency by influencing the amount of electrical power generated from the solar energy received. Consequently, improving these factors is essential for advancing solar technology and maximizing the potential of solar energy as a sustainable resource.

3. Conducting Polymers and Their Synthesis and Fabrication Techniques

Conducting polymers are a class of organic polymers known for their high electrical conductivity, making them highly valuable in solar cell applications. These polymers have conjugated molecular structures that facilitate efficient charge carrier transport. Due to their excellent conductivity, transparency, and compatibility with flexible substrates, conducting polymers are widely used as hole transport layers in various types of solar cells, including DSSCs, PSCs, and OSCs. Examples of commonly used conducting polymers include polyaniline (PANI), polypyrrole (PPy), poly(3-alkylthiophene) (P3aT), poly(3,4-ethylenedioxythiophene) (PEDOT), polyvinylpyrrolidone (PVP), poly(styrene sulfonate) (PSS), and poly(4-vinylpyridine) (P4VP) [38]. Their structures are depicted in Figure 5. The significance of these polymers lies in their ability to enhance the efficiency and stability of solar cells. In DSSCs, conducting polymers improve hole transport from dye molecules to the counter electrode, thereby enhancing charge separation and reducing recombination losses [43]. In perovskite solar cells, they can function as hole transport materials, anode buffer layers, or additives in the perovskite layer [44–46]. In organic solar cells, they are utilized in various device layers, including electron transport, hole transport, and active layers [47]. Thus, conducting polymers play a crucial role in advancing solar cell technologies, contributing to improved performance and broader applicability. Common methods for synthesizing conducting polymers, as illustrated in Figure 6, include chemical polymerization, electrochemical polymerization, in situ polymerization, emulsion polymerization, template-assisted polymerization, controlled radical polymerization, cross-coupling reactions, and Grignard-type metathesis polymerization. Subsequent sections will explore these polymerization methods in detail, focusing on their applications in counter electrodes, HTMs, electron transport materials, transparent conductive electrodes, active layers, dyes, and electrolytes.
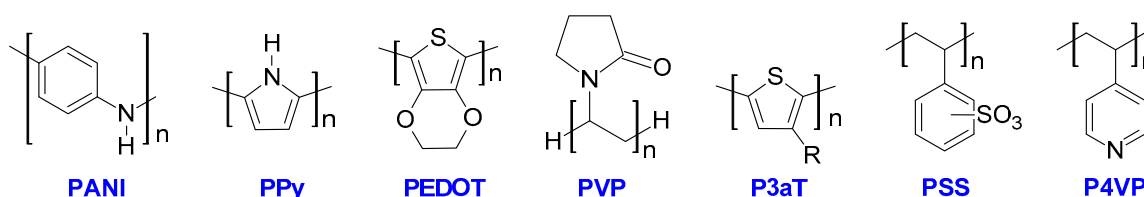

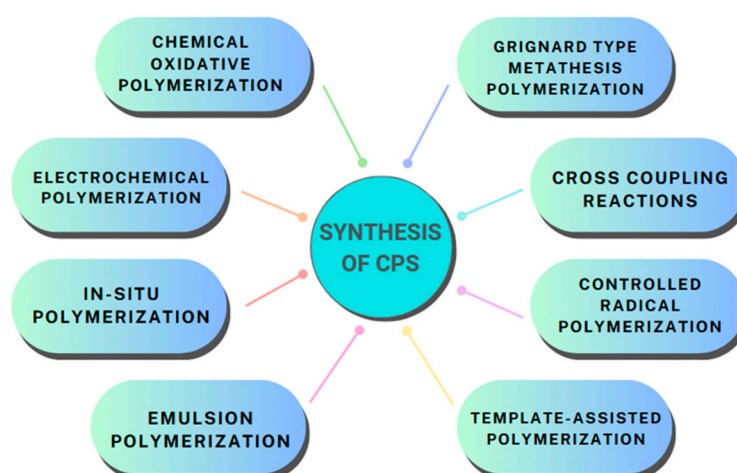**Figure 5.** Chemical structures of common polymers used in solar cells.

Figure 6. Common methods for synthesizing and fabricating conducting polymers.

3.1. Chemical Oxidative Polymerization

Chemical oxidative polymerization is a key method for synthesizing conducting polymers, offering significant advantages for their application such as the development of

cost-effective counter electrodes in dye-sensitized solar cells. This process involves the oxidation of a monomer to form a polymer, utilizing an oxidizing agent such as $FeCl_3$. This method has been particularly effective in producing poly(3,4-ethylenedioxythiophene), a polymer known for its superior electrocatalytic properties. For instance, PEDOT synthesized through chemical oxidative polymerization demonstrates exceptional performance as a counter electrode in DSSCs, outperforming traditional platinum-based electrodes. In a comparative study, a DSSC with a PEDOT-coated transparent conducting substrate as the counter electrode achieved a PCE of 7.88%, slightly surpassing the 7.65% PCE of a DSSC with a platinum-sputtered counter electrode. Electrochemical impedance spectroscopy (EIS) revealed that the PEDOT-based cell had lower charge-transfer resistance for the I^-/I_3^- redox reaction compared to its platinum counterpart. Furthermore, the electron transfer rate constant (k_0) for the I^-/I_3^- redox reaction was measured at 3.47×10^{-3} cm/s for the PEDOT electrode, which was higher than the 2.76×10^{-3} cm/s observed for the platinum electrode, despite similar electrode thickness and surface roughness [48].

Recent advancements have refined the synthesis of PEDOT through chemical oxidative polymerization. A notable method involves the use of anhydrous $FeCl_3$ to oxidize the monomer in acetonitrile, yielding a solid product that is then purified to minimize residue content to below 0.5%. The purified PEDOT is sonicated in water to create a stable aqueous dispersion, which can be concentrated up to 1.145 g/L and is stabilized by electrostatic repulsion. This conductive ink is subsequently applied to glass substrates using an air-brush technique, resulting in thin films that are both transparent and conductive. These films exhibit sheet resistances ranging from 1 to 20 kΩ/sq and transmittances of 50% to 80% at 550 nm, demonstrating the versatility and effectiveness of chemical oxidative polymerization in producing high-performance conducting films for various applications [49].

3.2. Electrochemical Polymerization

Electrochemical polymerization involves the process of forming polymers through an electrochemical reaction, typically occurring at an electrode interface. In the context of conducting polymers like PEDOT, this technique uses an electrical current to induce polymerization from a monomer solution. When applied to counter electrodes in dye-sensitized solar cells or as hole transport materials in perovskite solar cells, electrochemical polymerization offers precise control over the polymer's properties, such as thickness and conductivity.

For instance, the deposition of PEDOT on counter electrodes through this method significantly influences both the thickness and catalytic activity of the electrode. Using a scalable electropolymerization technique in a water-based sodium dodecyl sulfate (SDS) solution allows for the preparation of PEDOT films with controlled thicknesses by adjusting the polymerization time. This control is crucial for optimizing the performance of DSSCs, as different film thicknesses can affect the efficiency of the counter electrode's catalytic activity. Thicker PEDOT films, for example, were observed to have decreased catalytic efficiency, with the optimal thickness yielding a higher power conversion efficiency [50].

In perovskite solar cells, electrochemical polymerization is used to deposit PEDOT:PSS as a hole transport material. Adjusting the polymerization potential affects the charge carrier density of the HTM, impacting overall efficiency. Specifically, higher potentials can lead to overoxidation and reduced carrier density, which negatively affects performance. By carefully selecting lower synthesis potentials, a significant improvement in power conversion efficiency can be achieved [51].

Thus, electrochemical polymerization not only facilitates the precise fabrication of polymer films but also plays a pivotal role in enhancing solar cell performance by allowing tailored modifications of the polymer's properties.

3.3. In Situ Polymerization

In situ polymerization refers to the process of synthesizing polymers directly within a specific environment or matrix where the polymerization occurs. This technique is

employed to form polymers in their final location or configuration, allowing for precise control over the polymerization conditions and interactions with surrounding materials. By conducting polymerization reactions in place, this method ensures that the resulting polymers integrate seamlessly with their surroundings, which can significantly enhance material properties and performance.

For instance, in the development of solid-state electrolytes for DSSCs, in situ polymerization has proven to be an effective strategy. A novel approach involved creating an all-solid-state polymer electrolyte in situ using a thiolate/disulfide redox couple derived from a lamellar liquid crystal precursor. This technique preserved the lamellar nanostructure of the precursor, ensuring excellent interfacial contact between the electrolyte and the other components of the solar cell. Electrochemical analyses demonstrated that this method resulted in an electrolyte with charge transport and photovoltaic performance comparable to that of the original liquid crystal precursor. Notably, these all-solid-state DSSCs maintained stable performance with a power conversion efficiency exceeding 2% across a temperature range of 35 to 90 °C [52].

Another notable application of in situ polymerization is in the synthesis of polyaniline/polyvinylpyrrolidone blend electrolytes for DSSCs, which enhances their long-term stability. This process involves gradually adding aniline to a solution containing PVP and dodecylbenzenesulfonic acid (DBSA) (Figure 7), followed by the dropwise addition of ammonium persulfate in dimethylformamide. The resulting polymer blend gel electrolytes are uniform and homogeneous, making them well suited for use in DSSCs [53].
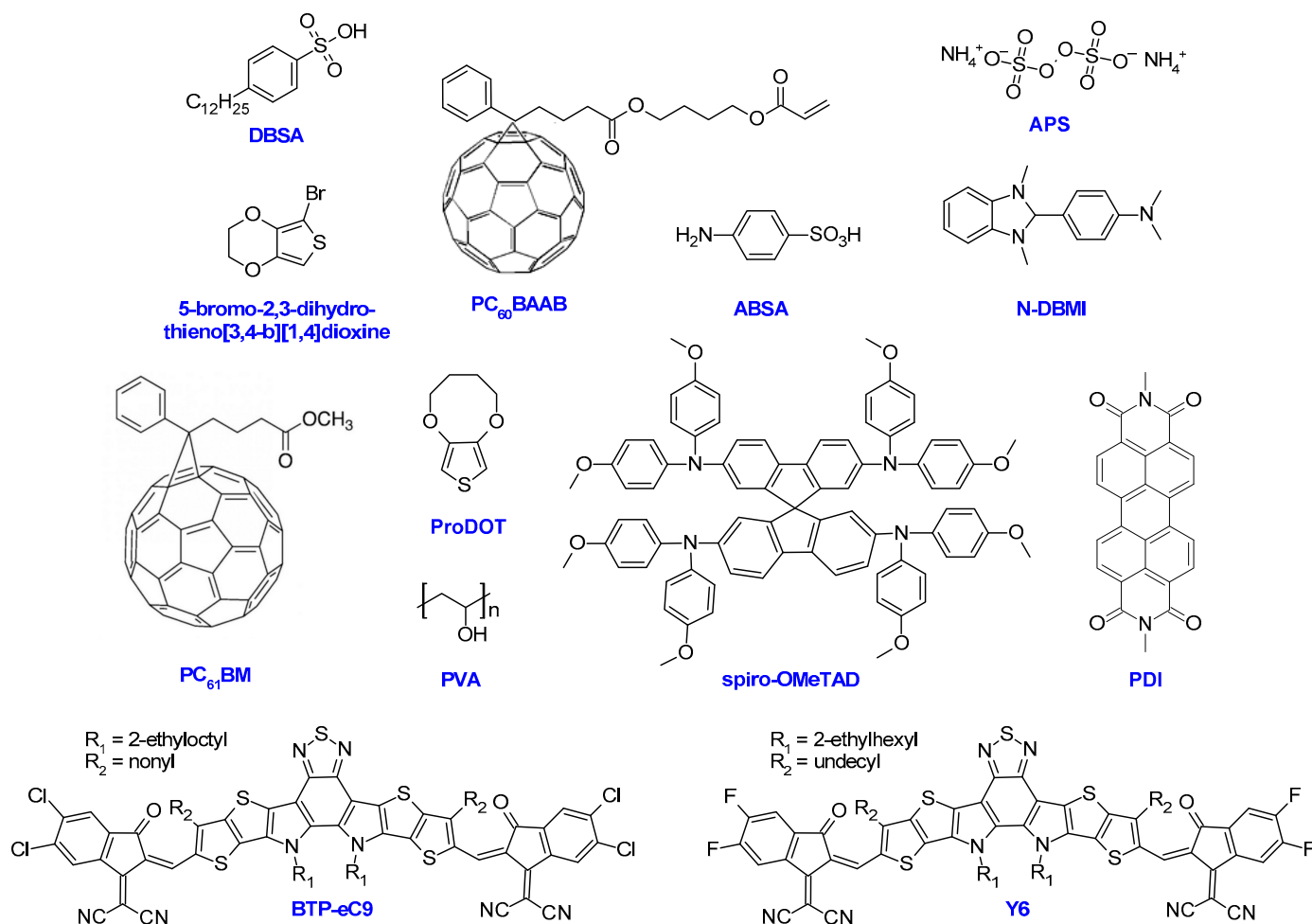

Figure 7. Chemical structures of the additives and acceptors discussed in this study.

In perovskite solar cells, in situ polymerization has been used to incorporate conducting polymers like PEDOT to improve efficiency and stability. In this process, the monomer 5-bromo-2,3-dihydrothieno[3,4-b][1,4]dioxine (Figure 7) is added directly to a perovskite precursor solution and polymerizes within the perovskite film during its formation. This approach aims to passivate surface and bulk defects, enhance charge extraction efficiency, and improve the film's resistance to thermal and moisture-related degradation [54].

Furthermore, in organic solar cells, the in situ photopolymerization of acrylate-based fullerides, like $PC_{60}BAAB$ (as illustrated in Figure 7), has been utilized to promote vertical phase separation within bulk heterojunctions. By irradiating the active layer with ultraviolet light, a gradient in UV intensity is created, which drives the diffusion of polymerizable monomers. This results in a polymer gradient and a counter gradient of unpolymerized monomers, leading to the formation of a continuous acceptor structure and improved power conversion efficiency of the solar cells [55].

Thus, in situ polymerization of conducting polymers is a versatile and effective approach for developing advanced materials in various types of solar cells. This method enhances performance, stability, and functionality by allowing precise control over polymer formation and integration within the final device structures.

3.4. Emulsion Polymerization

Emulsion polymerization is a versatile technique for synthesizing high-molecular-weight polymers. It involves dispersing monomers in a continuous aqueous phase to form an emulsion, where the monomers are encapsulated in small droplets. These droplets then undergo polymerization, leading to the formation of polymer particles suspended in the water phase. This method is favored for its ability to produce polymers with controlled properties and high molecular weights, as well as for its efficient heat and mass transfer. The process also eliminates the need for additional separation steps after polymerization.

Recent research has explored the use of conducting polymer electrolytes to enhance stability and performance. One significant study utilized emulsion polymerization to synthesize a novel conducting nanocomposite composed of polypyrrole and modified poly(styrene-alt-maleic anhydride) (PSMA) (as illustrated in Figure 8). This composite demonstrates high conductivity and effective heavy metal sorption capabilities. In the study, the emulsion polymerization process began by dispersing 1.5 g of PSMA-g-4ABSA, 2.65 g of dodecyl sulfate, and 20 mL of chloroform in 30 mL of distilled water using an ultrasonic bath for about one hour. Following this, 1 g of pyrrole monomer dissolved in 20 mL of 1 M hydrochloric acid was added to the mixture. An ammonium persulfate (APS) solution (20 mL, 0.435 M) was then added dropwise over 30 min under ultrasonic irradiation. The reaction proceeded at 0–5 °C for 24 h. The resulting black precipitate was filtered, washed with distilled water and acetone, and dried in a vacuum at 50 °C for 24 h. Emulsion polymerization was chosen for this synthesis due to its ability to produce high-molecular-weight polymers, provide precise control over the polymerization process, and ensure efficient heat and mass transfer. Additionally, this method allows for the direct use of the product without further separation. It is particularly useful for synthesizing active layers containing conducting polymers [56].

For instance, blend nanoparticles (NPs) were prepared using the Landfester mini-emulsion technique with minor adjustments [57]. A solution of $PC_{61}BM$ (Figure 7) and BCP5, which is based on a copolymer (poly[2,6-(4,4-bis-(2-ethylhexyl)-4H-cyclopenta[2,1-b;3,4-b′]dithiophene)-alt-4,7(2,1,3-benzothiadiazole)]) (PCPDTBT, structure shown in Figure 8) as the rigid block, was prepared in chloroform and stirred at room temperature for one hour. This mixture was then added to 1 mL of MilliQ water to create a macroemulsion, which was stirred for an additional hour. This macroemulsion was sonicated for 10 min at room temperature to produce a mini-emulsion, which was then heated to approximately 70 °C to remove the organic solvent, resulting in a stable aqueous suspension of the blend NPs. This emulsion polymerization technique is advantageous because it produces stable water-suspended blend NPs without requiring nonconducting surfactants, which can negatively

impact the performance of organic photovoltaic (OPV) devices. Additionally, it facilitates the creation of compact and uniform layers with adequate morphology for efficient charge percolation to the electrodes after mild annealing. This makes it a promising approach for the environmentally sustainable fabrication of OPV devices.
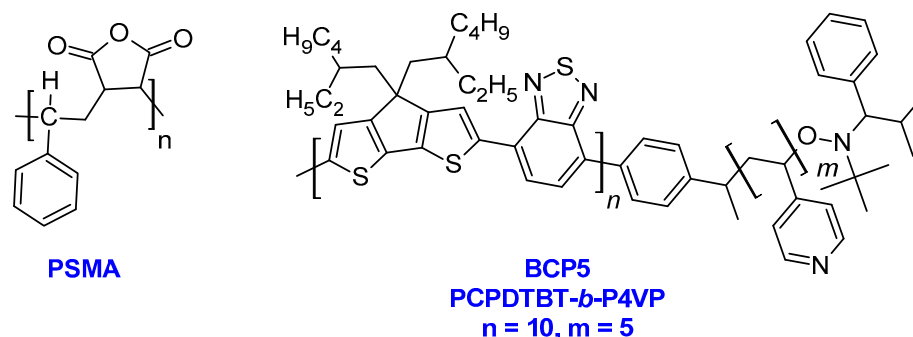
Figure 8. Chemical structures of PSMA and BCP5.

3.5. Template-Assisted Polymerization

Recent research has explored template-assisted polymerization as a method to enhance the properties of conducting polymers. This technique involves using templates to guide the polymerization process, which can significantly influence the final morphology and functionality of the resulting materials. In particular, azo dyes such as Acid Red 1, Orange G, and Sunset Yellow FCF have been employed as template agents to create organized supramolecular structures of polypyrrole in aqueous environments [58]. These dyes facilitate the formation of soft templates through self-assembly, which in turn directs the polymerization process, leading to the production of various nano- and microstructured forms of PPy, including rectangular nanotubes, plates, and barrel-like shapes. Template-assisted polymerization is critical as it allows for precise control over PPy's electrical properties and morphology, which is essential for applications in nanoscience and nanotechnology. The interactions between the azo dyes and the polymerization environment—including ionic and hydrogen bonding, π–π stacking, and hydrophobic interactions—play a crucial role in determining the final shape and properties of the synthesized PPy structures.

3.6. Controlled Radical Polymerization

Controlled radical polymerization (CRP) is a set of polymerization techniques that allow for better control over the molecular weight and distribution, architecture, and functionalization of polymers compared to traditional radical polymerization. The common types of CRP include atom transfer radical polymerization (ATRP) and reversible addition–fragmentation chain transfer (RAFT) polymerization that enable the precise control of polymer chains, making it easier to synthesize materials with specific properties [59].

ATRP involves the reversible transfer of halogen atoms, typically bromine or chlorine, between a dormant polymer chain and a transition metal catalyst, usually copper-based. ATRP provides good control over molecular weight and polymer architecture, enabling the synthesis of block copolymers and other complex structures under mild conditions. In contrast, RAFT polymerization utilizes a chain transfer agent (CTA) containing thioester or dithioester functionalities. The mechanism involves the reversible addition of a radical to the CTA, leading to a temporary intermediate that can fragment to form a new radical, perpetuating the polymerization process. RAFT relies on CTAs to mediate polymerization, allowing precise control over molecular weight and polydispersity. This method is particularly versatile, as it can be applied to a wider variety of monomers and is more tolerant of functional groups compared to ATRP [60].

3.7. Cross-Coupling Reactions

Cross-coupling reactions have become a powerful approach for synthesizing conducting polymers, enabling the formation of well-defined π-conjugated structures with a variety of functionalities. Techniques such as Stille, Suzuki, and direct arylation provide effective methods for polymerization [61]. A significant recent advancement is cross-dehydrogenative coupling polymerization, which allows the synthesis of alternating copolymers without the need for monomer pre-functionalization [62]. Palladium-catalyzed methods like Suzuki–Miyaura and Sonogashira coupling facilitate the production of conjugated polymers with tunable properties and high molecular weights [63–65]. Among these, direct (hetero)arylation polymerization (DHAP) stands out as an environmentally friendly alternative that forms C-C bonds between halogenated (hetero)arenes and simple (hetero)arenes with active C-H bonds [66,67]. DHAP has been successfully applied to various monomers, yielding nearly defect-free conjugated polymers [63]. Another recent development is cross-coupling polycondensation via C-O or C-N bond cleavage, which has broadened the range of suitable monomers [68]. These innovations have expanded the scope of π-conjugated polymers, which are increasingly used in organic electronics, including applications in solar cells, light-emitting diodes, and field-effect transistors [69].

3.8. Grignard-Type Metathesis Polymerization

Grignard-type metathesis polymerization (GRIM) is a valuable technique in the synthesis of conducting polymers, particularly within the framework of Kumada catalyst transfer polymerization (KCTP). It has garnered significant attention for its ability to produce high-quality conjugated polymers with precise control over molecular weight, regioregularity, and polymer structure. These advantages make it highly sought-after for applications in organic electronics, including photovoltaics, light-emitting diodes, and transistors [70]. A key advantage of GRIM lies in its use of magnesium-based Grignard reagents, which are highly reactive and enable the polymerization of a broad range of monomers, even those with challenging steric and electronic properties. In recent years, notable advancements have been made in optimizing the GRIM process. For instance, the use of water-scavenging Grignard reagents has significantly improved polymerization efficiency by preventing catalyst deactivation due to moisture exposure. This innovation has led to better control over polymerization kinetics and enhanced yields [71]. Additionally, researchers have explored combining different coupling reactions within the GRIM framework to modulate reactivity ratios in copolymerizations. This approach allows for more precise control over copolymer composition, enabling the tailoring of material properties for specific applications [72]. One notable application of GRIM polymerization is in the synthesis of conjugated block copolymers, such as regioregular poly(3-hexylthiophene). P3HT is extensively studied in organic electronics due to its favorable electronic properties, including good charge transport and high stability. The ability to control the regioregularity of P3HT through GRIM is crucial for achieving high-performance materials, as regioregular P3HT chains exhibit superior crystallinity and charge mobility compared to their irregular counterparts [73]. GRIM also facilitates the synthesis of well-defined block copolymers that can be used to optimize the morphology and performance of devices such as organic solar cells and organic field-effect transistors. By enabling the creation of high-quality, well-ordered conducting polymers, GRIM has significant potential to advance the development of next-generation organic electronic materials.

4. Optimizing Conducting Polymers for Solar Cells: Performance in Outdoor Conditions

4.1. Conducting Polymers in DSSCs

Conducting polymers are crucial for enhancing dye-sensitized solar cells, as they contribute to improved efficiency, stability, and cost-effectiveness. These polymers possess unique properties that make them well suited for multiple roles within DSSCs, such as counter electrodes, electrolytes, and dyes. Their application in these components highlights their pivotal role in advancing solar cell technology.

4.1.1. As Counter Electrodes

Polymer-based counter electrodes in solar cells are pivotal for dye regeneration as they facilitate electron acceptance from the external circuit. Comprising conducting polymers, these electrodes offer excellent electrical conductivity and catalytic activity [74]. Solar cells feature two primary electrodes: the anode, where oxidation occurs and electrons are lost, and the cathode, where reduction occurs, and electrons are gained. The cathode, or counter electrode, is especially crucial in dye-sensitized solar cells.

Polyaniline shows significant promise as a counter electrode in DSSCs due to its tunability through doping and distinct oxidation states. Research has highlighted its superior electrocatalytic activity compared to platinum counter electrodes, leading to higher efficiencies in DSSCs. PANI's porous structure enhances its ability to electrochemically reduce iodide ions, a key process in DSSCs. Consequently, solar cells with PANI counter electrodes achieved a PCE of 7.15%, surpassing the 6.90% efficiency of those using Pt [75]. Moreover, PANI's one-dimensional (1D) structure demonstrated superior electrocatalytic activity compared to both random-network PANI films and conventional Pt cathodes, leading to an increased short-circuit current density and fill factor. As a result, DSSCs with 1D PANI counter electrodes achieved an impressive efficiency of 8.24%, significantly higher than those using random-network PANI (5.97%) or Pt (6.78%) [75].

Polypyrrole, which is generally an insulator but becomes conductive when oxidized, also shows potential as a counter electrode in DSSCs. Synthesized PPy nanoparticles have exhibited high electrocatalytic activity, outperforming Pt-based counter electrodes by 11%. Thinner PPy films have achieved efficiencies of up to 6.8%. Composite materials, such as PPy mixed with carbon nanotubes, offer performance comparable to Pt-based counter electrodes, with efficiencies reaching up to 6.15%. These composite counter electrodes provide a promising pathway for creating efficient and cost-effective solar cells [76]. Research has also demonstrated high specific capacitance and excellent electrochemical performance of PPy electrodes in supercapacitors [77]. PPy nanosheets, with their high surface area and active sites, achieved a transmittance of 94% and a PCE of 6.8% in DSSCs, underscoring PPy's potential in various energy storage and conversion devices [78].

Polythiophene-based conjugated polymers are frequently used as electrodes in DSSCs. To enhance solubility and chemical stability, alkyl groups are often added. For example, a porous poly-3-methyl-thiophene (P3MT) was grown via electrochemical deposition for use as a counter electrode [79]. Incorporating materials like graphene or transition metals can further improve conductivity and catalytic activity. Polythiophene/graphene composites, for instance, achieved a PCE of 4.8%, while adding MoS_2 to bare thiophene reduced charge transfer resistance by 22%, leading to a 38% efficiency increase [80].

PEDOT has shown exceptional potential as a counter electrode in DSSCs since its initial use in 2002. PEDOT synthesized on conductive glass has demonstrated performance comparable to Pt-based counter electrodes in I^-/I_3^- based DSSCs [38]. PEDOT's performance can be optimized through the use of various monomer structures [81]. Recent research has explored PEDOT in neural interfacing and hybrid energy storage systems, highlighting its high capacitance and stability [81,82]. Among conjugated polymers commonly used as counter electrodes in DSSCs, PEDOT exhibits the highest efficiency. Furthermore, DMSO-treated PEDOT:PSS (with 0.1 wt.% carbon) achieved an efficiency of 5.81%, surpassing the reference electrode's PCE of 5.66% [83]. Similarly, DSSCs with MoS_2-GO/PEDOT:PSS counter electrodes achieved a notable power conversion efficiency of 7.73% under standard light conditions of 100 mW/cm^2, outperforming DSSCs with Pt-based counter electrodes, which had a lower efficiency of 5.53% [84].

4.1.2. As Electrolytes

Conducting polymers have emerged as promising alternatives to traditional liquid electrolytes in dye-sensitized solar cells, addressing stability and leakage issues [85,86]. Polymer electrolytes, such as blends of polyvinyl alcohol and PANI, offer improved long-term stability and electrode adhesion [53]. Gel polymer electrolytes (GPEs) have demon-

strated high ionic conductivity and durability [87], with some achieving conductivities up to 5.14 mS cm^{-1} [88]. By utilizing polyacrylonitrile as the matrix for the electrolyte, along with propylene carbonate (PC) as a plasticizer and varying amounts of tetrabutylammonium iodide (TBAI) and iodine, the researchers achieved a power conversion efficiency of 3.45% under optimized conditions. This improvement can be attributed to a high charge carrier density of 7.93×10^{20} cm^{-3}, which indicates enhanced charge transport and electron dynamics. These findings highlight the essential role of conducting polymers in advancing solar cell technology.

Another study investigated the impact of various plasticizers—specifically ethylene carbonate (EC), PC, γ-butyrolactone (GBL), and dibutyl phthalate (DBP)—on a polypyrrole-poly(vinyl alcohol)-based quasi-solid-state polymer electrolyte used in semi-transparent dye-sensitized solar cells [89]. Among these plasticizers, EC demonstrated enhanced conductivity, the lowest activation energy, and the lowest charge-transfer resistance. This enhancement was attributed to faster charge transfer occurring at the interface between the counter electrode and the electrolyte.

Novel materials, such as the dimedone-[N,N′-melaminium]propane sulfonate copolymer (PS, structure shown in Figure 9), represent a significant breakthrough in gel electrolytes [90]. PS, a nitrogen-rich polysulfobetaine-based gel, exhibits high ionic conductivity, measured at 6.8×10^{-3} S cm^{-1}. This conductivity has enabled notable achievements in dye-sensitized solar cells, with reported power conversion efficiencies reaching 6.26%. While slightly lower than the 7.07% PCE of its liquid electrolyte counterpart, these results highlight the potential of conducting polymers to enhance both performance and stability in DSSCs.
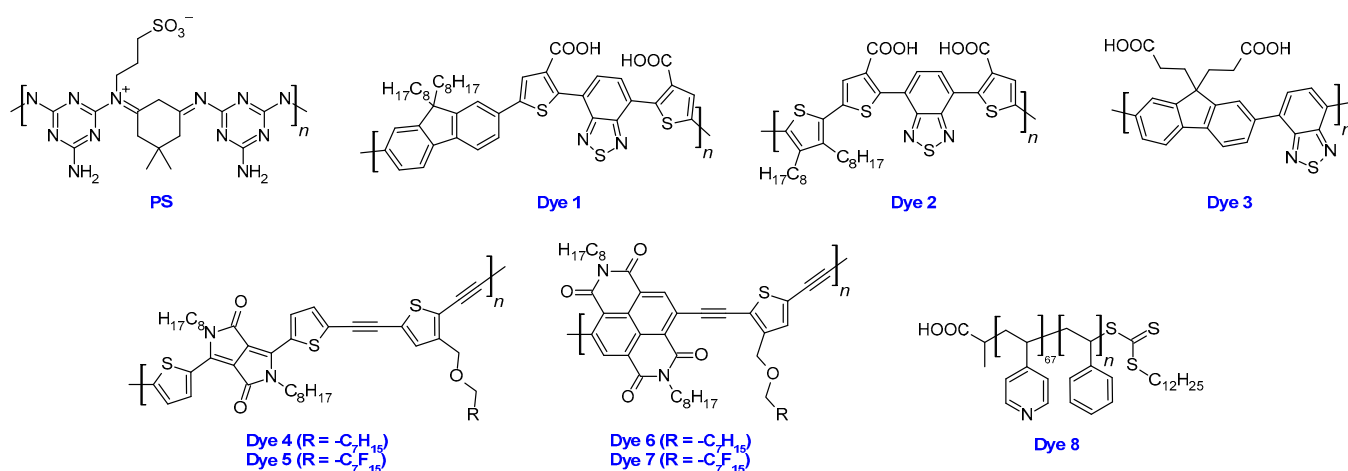
Figure 9. Chemical structures of some of the conducting polymers used in dye-sensitized solar cells.

PEDOT has proven to be an effective hole-transporting material in dye-sensitized solar cells (DSSCs). Notably, a significant power conversion efficiency of 6.1% was achieved with a fully organic D149 dye when PEDOT was used as the hole-transporting material. This result underscores the potential of PEDOT as a highly effective HTM in DSSCs.

4.1.3. As Dyes

Two conjugated polymers featuring carboxylic acid side groups were synthesized specifically for application in dye-sensitized solar cells, referred to as dyes 1 and 2, as depicted in Figure 9 [91]. These polymers demonstrate broad absorption across the visible spectrum, notably the dye 2 polymer which begins absorbing at approximately 625 nm. The most effective DSSC, utilizing a polymer with a molecular weight of 3980 Da (dye 2), achieved a peak incident photon-to-current conversion efficiency (IPCE) of about 65% and an overall power conversion efficiency of 2.99%. Interestingly, the efficiency of these solar cells showed an inverse relationship with the polymer's molecular weight, with shorter

chains exhibiting greater effectiveness in adsorbing onto TiO$_2$ surfaces. A related polymer, depicted in Figure 9 as dye 3, consists of a blend of polyfluorene and polybenzothiadiazole in a 7:3 ratio [92]. This polymer includes an anchoring moiety attached to the alkyl chains of the fluorene and is capable of absorbing light within the range of 280 to 510 nm. Despite this broad absorption spectrum, it only achieves a maximum PCE of 1.39%.

In a separate study, copolymers based on diketopyrrolopyrrole-thiophene (dyes 4 and 5) and perylenediimide (PDI)-thiophene (dyes 6 and 7) were investigated, with dyes 5 and 7 featuring a perfluoroalkyl side chain [93]. These dyes exhibit broad absorption bands spanning from 350 to 800 nm. The perylenediimide-thiophene copolymer dyes exhibit a bandgap that is approximately 0.34 eV lower than that of their diketopyrrolopyrrole-thiophene counterparts. Additionally, the introduction of a perfluoroalkyl side chain further reduces the bandgap by about 0.01 eV, leading to a slight red shift in their absorption spectra. The perylenediimide-thiophene copolymers resulted in a 21% increase in PCE, attributed to the red-shifted and broadened absorption spectrum and enhanced photogenerated electron injection into the TiO$_2$ conduction band, compared to the diketopyrrolopyrrole-thiophene systems. Additionally, the incorporation of perfluoroalkyl side chains (dyes 5 and 7) improved the PCE by about 8% relative to their non-perfluoroalkyl counterparts, as the favorable π–π stacking of the polymer chains created a more ordered microstructure at the donor–acceptor interface. This arrangement reduced charge recombination and provided additional driving forces for enhanced exciton dissociation at the TiO$_2$/dye/electrolyte interface.

Most conducting polymers used as dyes typically exhibit power conversion efficiencies below 3% [94–97]. To address this limitation, researchers have explored using conducting polymers as co-sensitizers to enhance efficiency. However, co-sensitization with multiple polymers often results in similarly low efficiencies [98]. A recent study employed a co-sensitization technique with block copolymers of poly(4-vinylpyridine) and poly(styrene) alongside the dye N719, as illustrated in Figure 9 (labeled as dye 8). By utilizing the RAFT polymerization process to control the chain lengths of the individual polymers, the authors produced a P4VP with 67 chains, combined with either 23 or 61 chains of poly(styrene), forming a copolymeric system. The PCE for N719 without co-sensitization was 5.1%, which increased to 6.7% when co-sensitized with P4VP alone. The copolymer containing 23 chains of poly(styrene) yielded a PCE of 7.6%, while the dye with 61 chains achieved a PCE of 7.4%. These improvements were attributed to increased open-circuit voltage and short-circuit current, along with reduced recombination reactions. In contrast, adding chenodeoxycholic acid (CDCA) to the system resulted in a PCE of 6.3%.

4.2. Conducting Polymers in PSCs

The utilization of conducting polymers in PSCs has introduced fresh opportunities to boost their performance, stability, and versatility. These polymers play crucial roles across different aspects of PSCs, serving as materials for transporting both holes and electrons, forming buffer layers, and creating transparent conductive electrodes. This section extensively examines the diverse contributions of conducting polymers, illustrating how they have been employed to enhance the efficiency, stability, and overall functionality of these devices.

4.2.1. As Hole Transport Materials

Conducting polymers have emerged as highly promising additives to enhance the performance and stability of perovskite solar cells. These polymers play critical roles in regulating crystallization, improving morphology, and passivating defects within perovskite films [45]. Specifically, they are being explored as effective hole transport materials in perovskite solar cells, offering significant advantages in terms of stability and performance. Various types of conducting polymers, such as polyaniline derivatives [99], PEDOT [46], and polypyrrole nanotubes [100], have been successfully utilized as HTMs in PSCs. These materials exhibit improved environmental stability, efficient hole extraction capabilities, and cost-effectiveness compared to traditional HTMs like spiro-OMeTAD [45].

PEDOT stands out among these conducting polymers due to its low cost, high conductivity, and ease of processing, making it particularly attractive for perovskite solar cells [46]. Recent studies have demonstrated promising results by combining dopant-free spiro-OMeTAD with water-free PEDOT, effectively passivating the perovskite/HTM interface and achieving high efficiencies [101]. Additionally, self-doped conducting polymers, such as PSS-g-PANI, have shown enhancements in built-in potential and device characteristics, further highlighting the versatility and potential of these materials in advanced photovoltaic applications [102].

Polythiophene-based materials have also shown considerable promise as HTMs in perovskite solar cells, improving both performance and stability. Ester-functionalized polythiophenes, for instance, enhance device efficiency and stability through Lewis-base passivation and improved charge transfer mechanisms [103]. Moreover, higher-molecular-weight variants of poly(3-hexylthiophene) have demonstrated superior photovoltaic performance, while doping P3HT with carbon nanostructures has been found to further enhance efficiency and stability in perovskite solar cells [104,105]. P3HT was employed as a dopant-free HTM in $CsPbI_3$, resulting in the highest reported power conversion efficiency of 17.92% [106].

Dopant-free hole transport materials mark a significant advancement in the development of perovskite solar cells, enhancing efficiency and stability while simplifying production and reducing costs. By removing the need for dopants—substances that can introduce variability and degrade long-term performance—these materials offer a more sustainable and reliable solution. Additionally, dopant-free hole transport materials tend to have better compatibility with the perovskite layer, which improves charge transport and minimizes recombination losses. This innovation is crucial for the commercialization of perovskite solar technology, as it facilitates scalable manufacturing and extends device longevity, ultimately supporting the broader adoption of renewable energy solutions.

Recently, two D-π-A-type polymers, HTM 1 and HTM 2, were utilized as dopant-free HTMs to enhance the PCE of $CsPbI_2Br$ perovskite solar cells, as illustrated in Figure 10 [107]. Among these, HTM 2, which features chlorinated thiophene side chains, exhibits superior molecular arrangement, energy level alignment, and passivation. As a result, it achieves a PCE of 17.60% and a notable V_{OC} of 1.44 V. The research also investigates the use of both HTMs in inter-connecting layers (ICLs) for tandem solar cells (TSCs), resulting in a PCE of 22.32% with HTM 2-ICL. The findings highlight that HTM 2 provides better surface passivation, reducing both radiative and non-radiative recombination losses, which significantly enhances the performance of both perovskite solar cells and TSCs.

In another study, researchers utilized a benzodithiophene-based backbone-conjugated polymer, referred to as HTM 3 (Figure 10), as a dopant-free hole transport material [108]. This innovative approach significantly enhances both the efficiency and stability of $CsPbI_3$ perovskite solar cells. The PSCs incorporating HTM 3 achieved a power conversion efficiency of 18.27%, outperforming those that employed the traditional Spiro-OMeTAD HTM. Additionally, HTM 3-based PSCs maintained over 90% of their initial power conversion efficiency after 3000 h in a nitrogen-filled glovebox, compared to only 80% retention for Spiro-OMeTAD-based PSCs. Moreover, HTM 3 enhances the moisture resistance of $CsPbI_3$ films, effectively preventing phase transitions and degradation.

One challenge in developing highly conjugated systems, such as CPs, is their solubility in environmentally friendly solvents. Addressing this concern, one study has successfully integrated the rigid structure of conjugated small-molecule components with a functionalized flexible backbone. This integration combines triphenylamine donors and a binaphthylamine core, forming a unique architecture with an extensive conjugated system, referred to as HTM 4, shown in Figure 10 [109]. HTM 4 has demonstrated high hole mobility and effective passivation of defects, achieving a remarkable efficiency of 20.23% in inverted perovskite solar cells. This performance surpasses that of the commercial polymer poly(triarylamine) (PTAA, see Figure 10). Furthermore, devices based on HTM 4 exhibited

enhanced long-term and thermal stability, retaining approximately 82% of their original PCE after 90 days in ambient air.
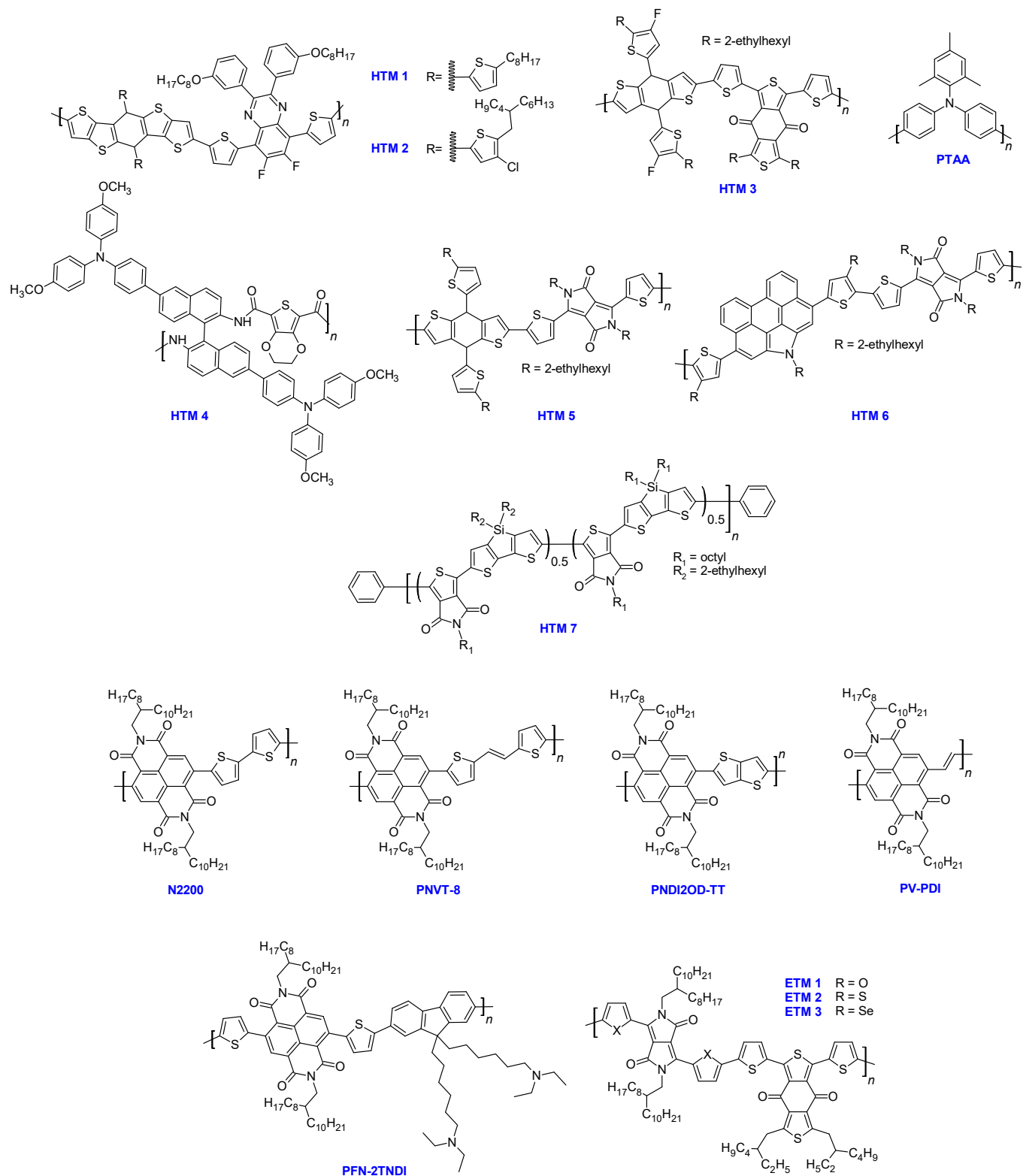

Figure 10. Chemical structures of some of the conducting polymers used in perovskite solar cells.

To improve charge transport in perovskite solar cells, researchers have focused on optimizing the molecular packing and orientation of dopant-free hole transport materials. In their study, they developed two conjugated polymers. The first, HTM 5, served as a control with a benzo[1,2-b:4,5-b′]dithiophene donor unit and a diketopyrrolopyrrole (DPP) acceptor unit (Figure 10). The second, HTM 6, replaced the donor unit with phenanthrocarbazole (PC-T). This alteration resulted in HTM 5 adopting an edge-on orientation, whereas HTM 6 preferred a face-on orientation of the polymer chains. Due to this optimized molecular structure, HTM 6 exhibited increased hole mobility and better interfacial contact with the perovskite surface. Consequently, these structural improvements led to a significant enhancement in device efficiency, with the dopant-free HTM 6-based device improving efficiency from 17.27% to 22.67% [110].

4.2.2. As Electron Transport Materials

Conducting polymers have emerged as highly promising materials for electron transport in perovskite solar cells, significantly improving both stability and performance [45]. Various perylenediimide-based polymers, including poly([N,N′-bis(2-octyldodecyl)-1,4,5,8-naphthalene diimide-2,6-diyl]-alt-5,5′-(2,2′-bithiophene)) (N2200), poly([N,N′-bis(alkyl)-1,4,5,8-naphthalene diimide-2,6-diyl-alt-5,5′-di(thiophen-2-yl)-2,2′-(E)-2-(2-(thiophen-2-yl)vinyl)thiophene]) (PNVT-8), and PNDI2OD-TT (structures are illustrated in Figure 10), have been explored using a spin-coating approach on substrates to ensure uniformity and consistency, which are crucial for efficient perovskite solar cell operation. Among these, N2200 has achieved a notable power conversion efficiency of 8.15% [31,111]. This demonstrates the effectiveness of conducting polymers as electron transport materials in inverted planar heterojunction perovskite solar cells. Additionally, doping semiconducting polymeric electron transport materials with n-type dopants can significantly enhance device performance. For instance, when N2200 is doped with 4-(1,3-dimethyl-2,3-dihydro-1*H*-benzoimidazol-2-yl)phenyl)dimethylamine (N-DBMI, Figure 6), the PCE doubles from 6.5% to 13.93% [112]. A simple addition of a vinyl moiety to the PVI, such as PV-PDI (Figure 10), has also shown promise, achieving a PCE of 10.14% [113]. Additionally, amino-functionalized conjugated polymers like PFN-2TNDI have surpassed traditional materials like PCBM, increasing the PCE from 12.9% to 16.7% [114].

Recent advancements also include the use of polymers as dopants to create uniform and compact electron transport layers due to the lowering of trap defects in the photo absorber and ETM, enhancing charge separation and transfer for efficient perovskite solar cell performance. A simple approach is the use of poly(acrylic acid) (PAA), which acts a buffering agent to stabilize SnO_2; this improved the PCE from 15.7% to 17.2% [115]. These developments underscore the potential of conducting polymers in enhancing the performance and stability of perovskite solar cells.

In another study, researchers developed and synthesized diketopyrrolopyrrole (DPP) and di-oxo-benzodithiophene (BDD) polymers flanked with furan, thiophene, and selenophene moieties (ETM 1 to 3, Figure 10) [116]. These polymers were employed both as anti-solvents and as dopants in PCBM within an inverted perovskite device configuration. When used as anti-solvents, all polymers exhibited higher fill factors compared to control PSCs. This improvement was attributed to reduced surface roughness, thereby minimizing defects at the perovskite layer surface. However, their J_{SC} slightly decreased, resulting in lower overall PCE values compared to the control devices. On the other hand, when the polymers were incorporated with PCBM, the polymer devices showed increased J_{SC} and FF. This enhancement was due to additional absorption in the near-infrared spectrum by the hybrid ETM structure and smoother surface morphology, resulting in higher PCE values compared to the control devices. Among the ETMs tested, ETM 1 achieved the highest PCE of 23.48%, closely followed by ETM 3 at 23.35% PCE. In contrast, the PCE for the control device stood at 22.83%.

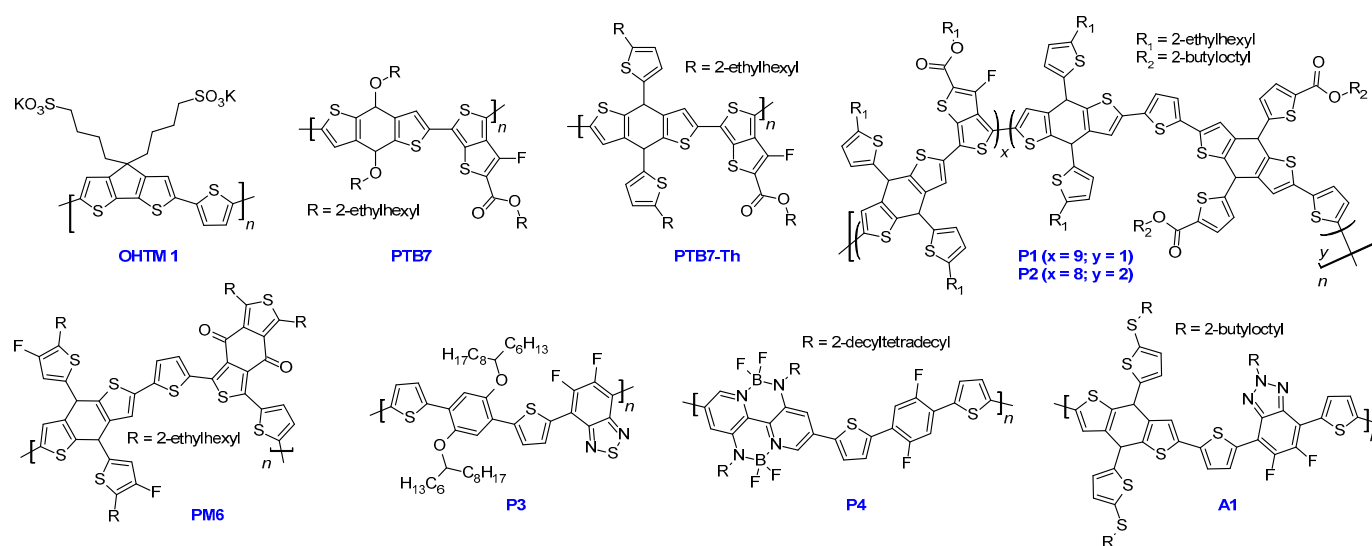### 4.3. Conducting Polymers in Organic Solar Cells

Conducting polymers serves as fundamental materials that facilitate charge transport within solar cell architecture. Their unique properties, including tunable electronic structures and excellent conductivity, enable effective movement of charge carriers, which is critical for optimizing the conversion of sunlight into electrical energy. These polymers can be engineered to achieve desired conductivity levels, absorption spectra, and energy levels, tailoring them for specific tasks within the cell. In the context of OSCs, the performance of these devices depends on the interaction between the active layer and various transport materials. The active layer, where light absorption and charge generation take place, relies on conducting polymers to enhance exciton dissociation and charge separation. This integration is important to maximize light absorption and ensure that the generated charges are collected efficiently.

4.3.1. As Hole Transport Materials

Conducting polymers are increasingly recognized for their potential as hole transport materials in organic solar cells, primarily due to their benefits including low-cost production, solution processability, and environmental friendliness [47,117]. Among these polymers, PEDOT and its derivatives have emerged prominently in both organic and perovskite solar cell technologies. Specifically, PEDOT:PSS is widely adopted as a hole transport material due to its high conductivity and transparency [118,119]. However, challenges such as its acidic nature and hygroscopic properties can compromise device stability. Researchers have explored various strategies to improve PEDOT's performance, such as incorporating organic solvents [120] or using lignosulfonate as a dopant [121]. A bilayer approach using two polymers can effectively enhance PCE and stability in OSCs. Brabec and colleagues employed PTAA and PEDOT:PSS as bilayer HTMs without the use of surfactants for all-solution-processed inverted OSCs featuring silver nanowire electrodes [122]. This bilayer hole transport layer achieved a PCE of 17.1%. Furthermore, it significantly improved operational stability, with devices maintaining 93% of their initial efficiency after 1800 h at 60 °C. This method is also well suited for industrial-scale production, utilizing solution-processing techniques and conventional materials like PEDOT:PSS.

Another approach involves replacing the acidic PSS with perfluorinated sulfonic acid ionomers as counterions (PEDOT:F) [123]. These ionomers can be dispersed in either water or alcohol, which facilitates their incorporation into various polymer matrices, enhancing compatibility and overall performance across a range of applications. This flexibility in solvent choice not only improves processing techniques but also allows for better control over material properties. PEDOT:F achieved a PCE of 16.28%, compared to only 12.37% for PEDOT:PSS. The reduced efficiency of solar cells using PEDOT:PSS is attributed to inadequate electrical contact, likely caused by energy level mismatches that occur after the addition of the surfactant, as well as the surfactant's aggregation on the surface of the active layer.

Polyaniline derivatives and conjugated polyelectrolytes (CPEs) have emerged as promising alternatives to PEDOT:PSS. These materials have shown enhanced stability, efficiency, and insensitivity to film thickness compared to PEDOT:PSS [124–126]. Particularly, CPEs with narrow bandgaps and high conductivity have demonstrated significant advancements in organic solar cell technology, achieving notable power conversion efficiencies of up to 9.3% [126]. This surpasses the performance of devices relying on PEDOT:PSS. One such polymer, labeled as OHTM-1 and illustrated in Figure 11, stands out for its composition featuring 3,4-dithia-7*H*-cyclopenta[a]pentalene and thienyl units. This polymer exhibits a self-doping effect, further enhancing its performance compared to PEDOT:PSS.

Figure 11. Chemical structures of some of the conducting polymers used in organic solar cells.

4.3.2. As Active Layers

Conducting polymers have become highly promising materials for active layers in organic solar cells thanks to their unique electronic properties and versatility. Adding a high-mobility conjugated polymer as an additive to the active layer can notably enhance the efficiency of these solar cells. Conjugated polymers, known for their favorable optical and electronic characteristics, are frequently employed as active layers in organic solar cells [127,128]. Semiconducting polymers, in particular, play a crucial role in improving the performance of such cells. PTB7 and its derivative PTB7-Th (structures presented in Figure 11) are recognized as the most effective polymer donors in organic solar cells, generating significant interest. However, its elevated HOMO level limits the V_{OC} of the organic solar cell devices, as a higher HOMO level can lead to reduced energy levels for electron extraction, ultimately constraining the voltage that can be achieved [129]. To enhance the open-circuit voltage, the study introduced a small quantity of poly(3-hexylthiophene) into the PTB7:PC$_{61}$BM active layers [130]. This addition enhances exciton dissociation and facilitates hole transport within the layers, leading to an increase in the V_{OC} to 0.84 V, up from a reference value of 0.74 V. This improvement significantly boosts the overall efficiency of the system. Furthermore, it is important to note that optimizing processing conditions, such as spin-coating speed and annealing temperature, can greatly affect device efficiency [131]. In another study, researchers aimed to optimize the open-circuit voltage by incorporating benzo[1,2-b:4,5-b′]dithiophene-2,6-dicarboxylate (VBDTC), a weak acceptor unit, into the PTB7-Th polymer. They synthesized two polymers by varying the PTB7-to-VBDTC ratio at 9:1 and 8:2, designated as P1 and P2, respectively, as shown in Figure 11 [132]. The addition of VBDTC to the PTB7 structure caused a blue shift in the absorption spectra, resulting in a decrease in J$_{SC}$. However, this modification also lowered the HOMO level, thereby enhancing the V_{OC}.

Certain polymers, such as P3 (structure presented in Figure 11), maintain high performance even in thick films due to their vertical carrier mobility and isotropic morphology [133]. Additionally, partially converted poly(1,4-phenylenevinylene) serves as a thin p-type interlayer in planar organohalide perovskite solar cells, achieving a high V_{OC} of 1.06 V, a power conversion efficiency of approximately 15%, and minimized charge carrier recombination [134].

The highest power conversion efficiency achieved for organic solar cell devices utilized the PM6 polymer as the donor (Figure 11) and BTP-eC9 as the acceptor (Figure 6). Additionally, a self-assembled molecule featuring phosphonic acid anchoring groups was used as the HTM, resulting in a PCE of 19.7% [14]. The researchers also compared the

results when using another common acceptor group, Y6 (Figure 6), which produced a PCE of 18.61%.

5. Optimizing Conducting Polymers for Solar Cells: Performance in Indoor Conditions

This section examines the indoor applications of conducting polymers in third-generation solar cells. Under typical indoor lighting conditions, which range from 200 to 2000 lux, a solar cell featuring a PEDOT-covered FTO counter electrode demonstrated optimal performance, achieving a peak efficiency of 28.9% at 1000 lux [135]. In 2018, researchers made a remarkable announcement of a major breakthrough in the field of solar technology. They achieved a new efficiency record for dye-sensitized solar cells specifically designed for indoor applications, achieving an impressive efficiency of 32% [136]. This surpassed the capabilities of even the most advanced silicon and gallium arsenide photovoltaic technologies available at that time. The cells also utilized a PEDOT counter electrode, marking a significant advancement in indoor solar energy generation. Further research using the Y123 dye and cobalt redox system examined the solar cell's performance across various light intensities from 200 to 1000 lux [137]. The study revealed that a PEDOT layer thickness of 90 nm was optimal, as it facilitated higher diffusivity, enhanced ionic conductivity, and reduced charge transfer resistance at the interface between the counter electrode and the electrolyte. Consequently, the PCEs recorded were 23.98% at 200 lux, 25.83% at 600 lux, and 26.93% at 1000 lux for a traditional DSSC photoelectrode comprising a main layer and a scattering layer. The remarkable performance of DSSCs indoors could signify a pivotal shift in the potential and adoption of photovoltaics.

Perovskite solar cells have emerged as promising candidates for indoor applications, particularly for powering Internet of Things (IoT) devices. However, when polymer-based hole transport materials are used, the polymer backbone often tends to twist, which reduces the perovskite–π-conjugation interaction. This twisting can lead to decreased carrier mobility and injection efficiency. To address this issue and enhance interchain π–π overlapping, researchers introduced a silole moiety into the thieno[3,4-c]pyrrole-4,6-dione structure, resulting in a dopant-free HTM designated as HTM 7 (Figure 10) [138]. HTM 7 demonstrated higher mobility compared to dopant-free P3HT devices and achieved an indoor PCE of 34.2% under 200 lux illumination.

Conducting polymers are well suited for indoor organic solar cell applications due to their tunable bandgaps, high absorption coefficients, and compatibility with low-light conditions. Recent advancements have led to power conversion efficiencies exceeding 20% under indoor lighting. Chemically synthesized PANI:PSS, used as a hole transport layer in organic solar cells for indoor applications, has demonstrated higher efficiency and stability compared to PEDOT:PSS, with over 90% transmittance and a work function of approximately 5.15 eV. Devices using this PANI film achieved around 10% power conversion efficiency under 1000-lux white LED light in indoor environments. Additionally, novel conjugated polymers incorporating thiazolothiazole and other units show promise for practical indoor applications, while strategies to enhance indoor organic solar cell performance include optimizing active layer thickness, improving dim light absorption, and integrating plasmonic metallic nanoparticles.

Researchers have developed an all-polymer configuration using a blend of two polymers: poly[4-(5-(4,8-bis(5-((2-butyloctyl)thio)thiophen-2-yl)-6-methylbenzo[1,2-b:4,5-b0]dithio-phen-2-yl)thiophen-2-yl)-5,6-difluoro-2-(2-hexyldecyl)-7-(5-methylthiophen-2-yl)-2H-benzo[d][1,2,3]triazole (P4) as the donor polymer, and poly[5,10-bis(2-decyltetradecyl)-2-(5-(2,5-difluoro-4-(5-methylthiophen-2-yl)phenyl)thio-phen-2-yl)-4,4,9,9-tetrafluoro-7-methyl-4,5,9,10-tetrahydro-3a,5,8a,10-tetraaza-4,9-diborapyrene-3a,8a-diium-5,11-diuide] (A1) as the acceptor polymer [139]. Their structures are illustrated in Figure 11. This P4:A1 blend achieved an impressive open-circuit voltage of 1.16 V, thanks to optimal energy alignment and an ideal bandgap of 1.93 V for indoor photovoltaics, resulting in a power conversion efficiency of 27.4%.

The highest reported power conversion efficiency in indoor organic solar cell devices has been achieved through the use of 2-(9*H*-carbazol-9-yl) phosphonic acid (2PACz) [22]. When incorporated into the processing of indium tin oxide and mixed with the active layer composed of PM6:Y6, this approach yielded an impressive efficiency of 36.3% under 1000 lux from an LED lamp. Notably, the device maintained 95% of its initial efficiency after 1000 h in ambient conditions. The integration of 2PACz significantly enhanced the carrier yield-mobility product, improved hole collection, and reduced trap-assisted recombination and transport losses. In contrast, control devices that did not use 2PACz achieved a PCE of only 25.5%.

6. Conducting Polymers in Transparent Conductive Electrodes

Conducting polymers, particularly PEDOT:PSS, have emerged as promising alternatives to traditional metal electrodes in perovskite solar cells. These polymers can serve as top electrodes, offering several advantages. PEDOT-based electrodes are notable for their solution processability, flexibility, and the ability to tune their color. They contribute to improved device stability, performance, and aesthetics by functioning as spectrally selective antireflection coatings. Composite electrodes, which combine conducting polymers with materials like silver nanowires, have demonstrated high transparency, low resistivity, and excellent mechanical flexibility [140–145]. Recent advancements in flexible electrodes, including those made from conductive polymers, have facilitated the development of efficient and bendable PSCs suitable for wearable and portable electronic applications [144]. In one study, PEDOT:PSS was successfully utilized as both top and bottom electrodes in PSCs, achieving power conversion efficiencies of 11.29% [140] and 14.5% [145].

Aside from PEDOT:PSS, researchers have also explored the use of p-type conjugated polymers. These polymers maintain an EDOT backbone, which gives them nearly identical optical properties to PEDOT:PSS while simultaneously improving electrical conductivities and using green solvents to facilitate large-scale production [146]. One notable example is the copolymerization of EDOT with a solubilizing agent, 3,4-propylenedioxythiophene (ProDOT), referred to as ProDOT-EDOT (Figure 12) [147]. Initially, researchers employed an ester derivative as the organic soluble precursor polymer, which was later converted into a water-based ink through base hydrolysis for efficient large-scale coating methods. Following coating, a dilute acid was applied to further functionalize the polymer film, imparting solvent resistance and compatibility with organic, aqueous, and biologically compatible electrolyte systems. This demonstrates the polymer's robustness under varying ionic conditions.
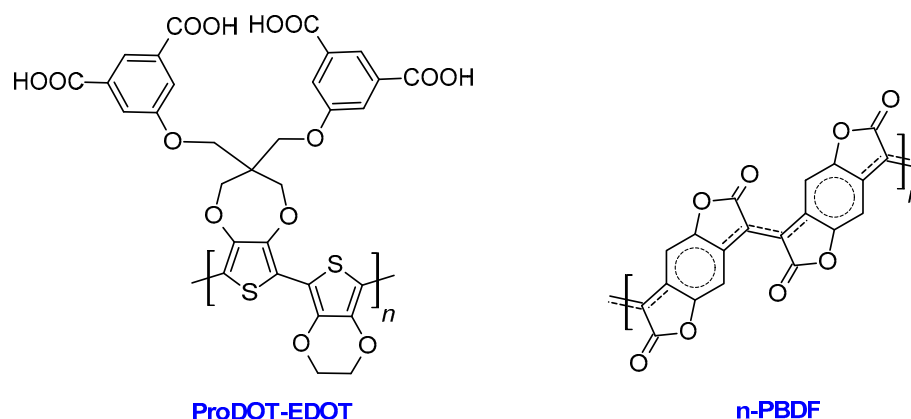
Figure 12. Chemical structures of ProDOT-EDOT and n-PBDF.

The n-type conjugated polymers, such as derivatives of poly(4-phenylenevinylene) and poly(benzimidazobenzophenanthroline), have been explored for use as transparent conductive electrodes. However, they typically face challenges such as low conductivity, insolubility, and poor doping efficiency, which hinder their practical implementation [146]. A recent

study introduced a polymer with an electron-deficient backbone, 7-dihydrobenzo[1,2-b:4,5-b′]difuran-2,6-dione (referred to as n-PBDF (Figure 12)), which exhibits several promising characteristics [148]. n-PBDF boasts the lowest HOMO level among all n-type conjugated polymers at −5.1 eV. Moreover, it demonstrates a low sheet resistance of 45 Ω/sq and achieves a transmittance of up to 80%, comparable to indium-doped transparent oxides. The ink formulation of n-PBDF remains stable on shelves and can be stored at temperatures ranging from −20 to 65 °C. Its work function ranges from 4.4 to 4.6 eV, and it exhibits stability against air, moisture, and heat. These attributes mark a significant breakthrough in the development of n-type polymers for this application.

7. Challenges and Future Outlook for Conducting Polymers

Conducting polymers hold significant promise in various applications, yet challenges remain in optimizing their use in devices such as dye-sensitized, perovskite, and organic solar cells.

To enhance the stability, efficiency, and overall viability of DSSCs, it is crucial to refine material selection, fabrication techniques, and performance evaluation. For instance, while polyaniline serves as a counter electrode, its power conversion efficiency is typically lower compared to platinum-based DSSCs. However, improvements can be made through the use of ternary composites like Ni–PANI–graphene [149] or by doping PANI with surfactants [150]. Additionally, polypyrrole counter electrodes face challenges related to high charge transfer resistance and limited conductivity, which are influenced by synthesis methods, morphology, and doping types [38]. Polythiophene, on the other hand, suffers from performance limitations due to its film thickness, which can adversely affect efficiency [151]. Although poly(3,4-ethylenedioxythiophene) is a viable counter electrode, prolonged exposure to air can degrade its molecular structure, leading to decreased electrical conductivity as the ratios of insulating to conducting components change. To address these issues, integrating polymer-based counter electrodes into composite materials may enhance performance by leveraging synergies with other components. Furthermore, there is a notable lack of research on the use of polymer-based counter electrodes in indoor applications of DSSCs, highlighting the need for further investigation to fully realize their potential.

In contrast, perovskite solar cells have rapidly gained attention as a promising photovoltaic technology, with efficiencies soaring from 3.8% to 28.8% over the past decade. PSCs offer several advantages, including low fabrication costs, tunable bandgaps, and excellent charge transport properties. However, their commercialization is hindered by challenges such as instability in moisture, oxygen, and UV light, lead toxicity, and hysteresis in current–voltage measurements. Researchers are actively exploring various strategies to overcome these hurdles, including the development of lead-free alternatives, improved fabrication techniques, and novel device architectures. Tunability and transparency are two of the properties that need to be carefully controlled in conducting polymers for applications like solar cells and organic electronic devices. The tunability of these polymers is largely determined by factors such as molecular weight, chain length, and the presence of specific side chains and functional groups [152]. For example, poly(3-alkylthiophenes), particularly poly(3-hexylthiophene), can have their properties finely adjusted by modifying the length and structure of their alkyl side chains. These modifications impact the polymer's molecular packing, absorption characteristics, and compatibility with other materials, allowing for optimization of device efficiency and stability [153]. Transparency, on the other hand, is crucial for applications where light transmission is essential, such as in solar cells and displays. The transparency of conducting polymers is primarily influenced by their optical bandgap and film thickness. Poly(3,4-ethylenedioxythiophene), for example, is known for its high transparency in the visible spectrum due to its wide optical bandgap, making it ideal for use as a transparent electrode in optoelectronic devices. By adjusting film thickness during deposition, both conductivity and transparency can be optimized to suit specific device requirements [154].

Similarly, organic solar cells present numerous advantages such as low cost, flexibility, lightweight design, and the potential for large-area fabrication. Recent advancements have improved their power conversion efficiencies, reaching up to 19.7% in binary devices. OSCs are particularly promising for applications in greenhouse-integrated photovoltaics, wearable electronics, and building integration. However, they continue to face challenges related to device stability, which impacts their commercial viability. Key stability factors include metastable morphology, diffusion of electrodes and buffer layers, and environmental stressors like oxygen, water, and irradiation. Ongoing research aims to improve efficiency through strategies such as bandgap tuning, morphology control, and innovative material design. Despite these challenges, OSCs have the potential to emerge as one of the most cost-effective and environmentally friendly forms of electricity generation, underscoring the need for continued research to unlock their full capabilities.

Author Contributions: Conceptualization, visualization, and formal analysis, A.Y. and M.P.B.; investigation, data curation, and writing—original draft preparation, A.Y., S.D.B. and B.B.; supervision, project administration, and funding acquisition, B.B. and M.P.B.; writing—review and editing, M.P.B. All authors have read and agreed to the published version of the manuscript.

Data Availability Statement: The original contributions presented in the study are included in the article; further inquiries can be directed to the corresponding authors.

Conflicts of Interest: The authors declare no conflicts of interest.

References

1. Chanthakett, A.; Arif, M.T.; Khan, M.M.K.; Subhani, M. Chapter 4—Hydrogen production from municipal solid waste using gasification method. In *Hydrogen Energy Conversion and Management*; Khan, M.M.K., Azad, A.K., Oo, A.M.T., Eds.; Elsevier: Amsterdam, The Netherlands, 2024; pp. 103–131.
2. Bosch, J.; Staffell, I.; Hawkes, A.D. Temporally explicit and spatially resolved global offshore wind energy potentials. *Energy* **2018**, *163*, 766–781. [CrossRef]
3. Thaker, M.; Zambre, A.; Bhosale, H. Wind farms have cascading impacts on ecosystems across trophic levels. *Nat. Ecol. Evol.* **2018**, *2*, 1854–1858. [CrossRef] [PubMed]
4. Zarfl, C.; Berlekamp, J.; He, F.; Jähnig, S.C.; Darwall, W.; Tockner, K. Future large hydropower dams impact global freshwater megafauna. *Sci. Rep.* **2019**, *9*, 18531. [CrossRef] [PubMed]
5. Idroes, G.M.; Hardi, I.; Hilal, I.S.; Utami, R.T.; Noviandy, T.R.; Idroes, R. Economic growth and environmental impact: Assessing the role of geothermal energy in developing and developed countries. *Innov. Green Dev.* **2024**, *3*, 100144. [CrossRef]
6. Odzijewicz, J.I.; Wołejko, E.; Wydro, U.; Wasil, M.; Jabłońska-Trypuć, A. Utilization of ashes from biomass combustion. *Energies* **2022**, *15*, 9653. [CrossRef]
7. Kabir, E.; Kumar, P.; Kumar, S.; Adelodun, A.A.; Kim, K.-H. Solar energy: Potential and future prospects. *Renew. Sust. Energ. Rev.* **2018**, *82*, 894–900. [CrossRef]
8. Soonmin, H.; Hardani; Nandi, P.; Mwankemwa, B.S.; Malevu, T.D.; Malik, M.I. Overview on different types of solar cells: An update. *Appl. Sci.* **2023**, *13*, 2051. [CrossRef]
9. Pastuszak, J.; Węgierek, P. Photovoltaic cell generations and current research directions for their development. *Materials* **2022**, *15*, 5542. [CrossRef]
10. Saranya, K.; Rameez, M.; Subramania, A. Developments in conducting polymer based counter electrodes for dye-sensitized solar cells—An overview. *Eur. Polym. J.* **2015**, *66*, 207–227. [CrossRef]
11. Aldamasy, M.; Iqbal, Z.; Li, G.; Pascual, J.; Alharthi, F.; Abate, A.; Li, M. Challenges in tin perovskite solar cells. *Phys. Chem. Chem. Phys.* **2021**, *23*, 23413–23427. [CrossRef]
12. Shi, Z.; Jayatissa, A.H. Perovskites-based solar cells: A review of recent progress, materials and processing methods. *Materials* **2018**, *11*, 729. [CrossRef] [PubMed]
13. Devadiga, D.; Selvakumar, M.; Shetty, P.; Santosh, M.S. Dye-sensitized solar cell for indoor applications: A mini-review. *J. Electron. Mater.* **2021**, *50*, 3187–3206. [CrossRef]
14. Yu, X.; Ding, P.; Yang, D.; Yan, P.; Wang, H.; Yang, S.; Wu, J.; Wang, Z.; Sun, H.; Chen, Z.; et al. Self-assembled molecules with asymmetric backbone for highly stable binary organic solar cells with 19.7 % efficiency. *Angew. Chem. Int. Ed.* **2024**, *63*, e202401518. [CrossRef] [PubMed]

15. Green, M.A.; Dunlop, E.D.; Yoshita, M.; Kopidakis, N.; Bothe, K.; Siefer, G.; Hao, X. Solar cell efficiency tables (Version 63). *Prog. Photovoltaics Res. Appl.* **2024**, *32*, 3–13. [CrossRef]

16. Li, C.; Chen, L.; Jiang, F.; Song, Z.; Wang, X.; Balvanz, A.; Ugur, E.; Liu, Y.; Liu, C.; Maxwell, A.; et al. Diamine chelates for increased stability in mixed Sn–Pb and all-perovskite tandem solar cells. *Nat. Energy* **2024**, *9*, 1388–1396. [CrossRef]

17. Ren, Y.; Zhang, D.; Suo, J.; Cao, Y.; Eickemeyer, F.T.; Vlachopoulos, N.; Zakeeruddin, S.M.; Hagfeldt, A.; Grätzel, M. Hydroxamic acid pre-adsorption raises the efficiency of cosensitized solar cells. *Nature* **2023**, *613*, 60–65. [CrossRef] [PubMed]

18. Mozaffari, S.; Nateghi, M.R.; Zarandi, M.B. An overview of the challenges in the commercialization of dye sensitized solar cells. *Renew. Sust. Energ. Rev.* **2017**, *71*, 675–686. [CrossRef]

19. Rahman, S.; Haleem, A.; Siddiq, M.; Hussain, M.K.; Qamar, S.; Hameed, S.; Waris, M. Research on dye sensitized solar cells: Recent advancement toward the various constituents of dye sensitized solar cells for efficiency enhancement and future prospects. *RSC Adv.* **2023**, *13*, 19508–19529. [CrossRef]

20. Park, J.; Kim, J.; Yun, H.-S.; Paik, M.J.; Noh, E.; Mun, H.J.; Kim, M.G.; Shin, T.J.; Seok, S.I. Controlled growth of perovskite layers with volatile alkylammonium chlorides. *Nature* **2023**, *616*, 724–730. [CrossRef]

21. Venkatesan, S.; Hsu, T.-H.; Teng, H.; Lee, Y.-L. Dye-sensitized solar cells with efficiency over 36% under ambient light achieved by cosensitized tandem structure. *Solar RRL* **2023**, *7*, 2300220. [CrossRef]

22. Kim, T.H.; Park, N.W.; Saeed, M.A.; Jeong, S.Y.; Woo, H.Y.; Park, J.; Shim, J.W. Record indoor performance of organic photovoltaics with long-term stability enabled by self-assembled monolayer-based interface management. *Nano Energy* **2023**, *112*, 108429. [CrossRef]

23. Dong, C.; Li, X.-M.; Ma, C.; Yang, W.-F.; Cao, J.-J.; Igbari, F.; Wang, Z.-K.; Liao, L.-S. Lycopene-Based Bionic Membrane for Stable Perovskite Photovoltaics. *Adv. Funct. Mater.* **2021**, *31*, 2011242. [CrossRef]

24. Qiu, C.; Wu, Y.; Song, J.; Wang, W.; Li, Z. Efficient planar perovskite solar cells with ZnO electron transport layer. *Coatings* **2022**, *12*, 1981. [CrossRef]

25. Sum, T.C.; Mathews, N. Advancements in perovskite solar cells: Photophysics behind the photovoltaics. *Energy Environ. Sci.* **2014**, *7*, 2518–2534. [CrossRef]

26. Jung, H.S.; Park, N.-G. Perovskite solar cells: From materials to devices. *Small* **2015**, *11*, 10–25. [CrossRef]

27. Fujiwara, H.; Kato, M.; Tamakoshi, M.; Miyadera, T.; Chikamatsu, M. Optical characteristics and operational principles of hybrid perovskite solar cells. *Phys. Status Solidi A* **2018**, *215*, 1700730. [CrossRef]

28. Gonzalez-Pedro, V.; Juarez-Perez, E.J.; Arsyad, W.-S.; Barea, E.M.; Fabregat-Santiago, F.; Mora-Sero, I.; Bisquert, J. General working principles of $CH_3NH_3PbX_3$ perovskite solar cells. *Nano Lett.* **2014**, *14*, 888–893. [CrossRef]

29. Hsiao, Y.-C.; Wu, T.; Li, M.; Liu, Q.; Qin, W.; Hu, B. Fundamental physics behind high-efficiency organo-metal halide perovskite solar cells. *J. Mater. Chem. A* **2015**, *3*, 15372–15385. [CrossRef]

30. Ghosh, P.; Sundaram, S.; Nixon, T.P.; Krishnamurthy, S. Influence of nanostructures in perovskite solar cells. In *Encyclopedia of Smart Materials*; Olabi, A.-G., Ed.; Elsevier: Oxford, UK, 2022; pp. 646–660.

31. Baptayev, B.; Tashenov, Y.; Balanay, M.P. Conjugated Polymers as Organic Electrodes for Photovoltaics. In *Organic Electrodes: Fundamental to Advanced Emerging Applications*; Gupta, R.K., Ed.; Springer International Publishing: Cham, Switzerland, 2022; pp. 137–153.

32. Wei, W.; Wang, H.; Hu, Y.H. A review on PEDOT-based counter electrodes for dye-sensitized solar cells. *Int. J. Energy Res.* **2014**, *38*, 1099–1111. [CrossRef]

33. Theerthagiri, J.; Senthil, A.R.; Madhavan, J.; Maiyalagan, T. Recent progress in non-platinum counter electrode materials for dye-sensitized solar cells. *ChemElectroChem* **2015**, *2*, 928–945. [CrossRef]

34. Noman, M.; Khan, Z.; Jan, S.T. A comprehensive review on the advancements and challenges in perovskite solar cell technology. *RSC Adv.* **2024**, *14*, 5085–5131. [CrossRef] [PubMed]

35. Prajapat, K.; Dhonde, M.; Sahu, K.; Bhojane, P.; Murty, V.V.S.; Shirage, P.M. The evolution of organic materials for efficient dye-sensitized solar cells. *J. Photochem. Photobiol. C* **2023**, *55*, 100586. [CrossRef]

36. Fu-Quan, B.; Wei, L.; Hong-Xing, Z. Theoretical studies of titanium dioxide for dye-sensitized solar cell and photocatalytic reaction. In *Titanium Dioxide*; Magdalena, J., Ed.; IntechOpen: Rijeka, Croatia, 2017; Chapter 10.

37. Schuster, C.S.; Morawiec, S.; Mendes, M.J.; Patrini, M.; Martins, E.R.; Lewis, L.; Crupi, I.; Krauss, T.F. Plasmonic and diffractive nanostructures for light trapping—An experimental comparison. *Optica* **2015**, *2*, 194–200. [CrossRef]

38. Ding, S.; Yang, C.; Yuan, J.; Li, H.; Yuan, X.; Li, M. An overview of the preparation and application of counter electrodes for DSSCs. *RSC Adv.* **2023**, *13*, 12309–12319. [CrossRef]

39. Yip, H.-L.; Jen, A.K.Y. Recent advances in solution-processed interfacial materials for efficient and stable polymer solar cells. *Energy Environ. Sci.* **2012**, *5*, 5994–6011. [CrossRef]

40. Duan, L.; Uddin, A. Progress in stability of organic solar cells. *Adv. Sci.* **2020**, *7*, 1903259. [CrossRef]

41. Sudhakar, Y.N.; Selvakumar, M.; Bhat, D.K. Chapter 4—Biopolymer electrolytes for solar cells and electrochemical cells. In *Biopolymer Electrolytes*; Sudhakar, Y.N., Selvakumar, M., Bhat, D.K., Eds.; Elsevier: Amsterdam, The Netherlands, 2018; pp. 117–149.

42. Abdulrazzaq, O.A.; Saini, V.; Bourdo, S.; Dervishi, E.; Biris, A.S. Organic solar cells: A review of materials, limitations, and possibilities for improvement. *Part. Sci. Technol.* **2013**, *31*, 427–442. [CrossRef]

43. Hou, W.; Xiao, Y.; Han, G.; Lin, J.-Y. The applications of polymers in solar cells: A review. *Polymers* **2019**, *11*, 143. [CrossRef] [PubMed]

44. Ahn, S.; Jeong, S.-H.; Han, T.-H.; Lee, T.-W. Conducting polymers as anode buffer materials in organic and perovskite optoelectronics. *Adv. Opt. Mater.* **2017**, *5*, 1600512. [CrossRef]

45. Girish, K.H.; Vishnumurthy, K.A.; Roopa, T.S. Role of conducting polymers in enhancing the stability and performance of perovskite solar cells: A brief review. *Mater. Today Sustain.* **2022**, *17*, 100090. [CrossRef]

46. Jiang, X.; Yu, Z.; Zhang, Y.; Lai, J.; Li, J.; Gurzadyan, G.G.; Yang, X.; Sun, L. High-performance regular perovskite solar cells employing low-cost poly(ethylenedioxythiophene) as a hole-transporting material. *Sci. Rep.* **2017**, *7*, 42564. [CrossRef]

47. Kumar, V.; Jule, L.T.; Ramaswamy, K. Conducting Polymers for Organic Solar Cell Applications. In *Conducting Polymers for Advanced Energy Applications*, 1st ed.; Gupta, R.K., Ed.; CRC Press: Boca Raton, FL, USA, 2021; pp. 139–151.

48. Machida, K.; Koseki, K.; Takeuchi, S. Electrochemical investigation of PEDOT counter electrode for dye-sensitized solar cells. *Electrochemistry* **2022**, *90*, 017003. [CrossRef]

49. das Neves, M.F.F.; Damasceno, J.P.V.; Junior, O.D.L.; Zarbin, A.J.G.; Roman, L.S. Conductive ink based on PEDOT nanoparticles dispersed in water without organic solvents, passivant agents or metallic residues. *Synth. Met.* **2021**, *272*, 116657. [CrossRef]

50. Pradhan, S.C.; Soman, S. Effect of thickness on charge transfer properties of conductive polymer based PEDOT counter electrodes in DSSC. *Results Surf. Interfaces* **2021**, *5*, 100030. [CrossRef]

51. Erazo, E.A.; Ortiz, P.; Cortés, M.T. Tailoring the PEDOT:PSS hole transport layer by electrodeposition method to improve perovskite solar cells. *Electrochim. Acta* **2023**, *439*, 141573. [CrossRef]

52. Li, X.; Zhao, Z.; Zhou, J.; Wang, C.; Wu, Y.; Tan, S. An all-solid-state lamellar-nanostructured polymer electrolyte in-situ-prepared from smectic liquid crystal for thermally stable dye-sensitized solar cells. *Chem. Eng. Sci.* **2020**, *221*, 115710. [CrossRef]

53. Yasmeen, S.; Gill, Y.Q.; Nazar, R.; Mehmood, U.; Iqbal, F.; Qaswar, H.; Ahmed, Z. Quasi-solid polyaniline/poly(vinyl pyrrolidone) blend electrolytes for dye-sensitized solar cells. *Mater. Chem. Phys.* **2023**, *305*, 128025. [CrossRef]

54. Gu, W.-M.; Jiang, K.-J.; Zhang, Y.; Yu, G.-H.; Gao, C.-Y.; Fan, X.-H.; Yang, L.-M. In-Situ polymerization of PEDOT in perovskite thin films for efficient and stable photovoltaics. *Chem. Eng. J.* **2022**, *430*, 133109. [CrossRef]

55. Zhang, L.; Xing, X.; Zheng, L.; Chen, Z.; Xiao, L.; Qu, B.; Gong, Q. Vertical phase separation in bulk heterojunction solar cells formed by in situ polymerization of fulleride. *Sci. Rep.* **2014**, *4*, 5071. [CrossRef]

56. Nazarzadeh Zare, E.; Mansour Lakouraj, M.; Najafi Moghadam, P.; Hasanzadeh, R. Novel conducting nanocomposite based on polypyrrole and modified poly(styrene-alt-maleic anhydride) via emulsion polymerization: Synthesis, Characterization, Antioxidant, and heavy metal sorbent activity. *Polym. Compos.* **2015**, *36*, 138–144. [CrossRef]

57. Zappia, S.; Scavia, G.; Ferretti, A.M.; Giovanella, U.; Vohra, V.; Destri, S. Water-processable amphiphilic low band gap block copolymer:fullerene blend nanoparticles as alternative sustainable approach for organic solar cells. *Adv. Sustain. Syst.* **2018**, *2*, 1700155. [CrossRef]

58. Valtera, S.; Prokeš, J.; Kopecká, J.; Vrňata, M.; Trchová, M.; Varga, M.; Stejskal, J.; Kopecký, D. Dye-stimulated control of conducting polypyrrole morphology. *RSC Adv.* **2017**, *7*, 51495–51505. [CrossRef]

59. Maity, N.; Dawn, A. Conducting polymer grafting: Recent and key developments. *Polymers* **2020**, *12*, 709. [CrossRef] [PubMed]

60. Truong, N.P.; Jones, G.R.; Bradford, K.G.E.; Konkolewicz, D.; Anastasaki, A. A comparison of RAFT and ATRP methods for controlled radical polymerization. *Nat. Rev. Chem.* **2021**, *5*, 859–869. [CrossRef] [PubMed]

61. Koizumi, T.-a.; Kanbara, T. Cross-Coupling Polymerization. In *Organometallic Reactions and Polymerization*; Osakada, K., Ed.; Springer: Berlin/Heidelberg, Germany, 2014; pp. 271–301.

62. Chakraborty, B.; Luscombe, C.K. Cross-Dehydrogenative Coupling Polymerization via C−H Activation for the Synthesis of Conjugated Polymers. *Angew. Chem. Int. Ed.* **2023**, *62*, e202301247. [CrossRef] [PubMed]

63. Jiang, K.; Zhang, L.; Zhao, Y.; Lin, J.; Chen, M. Palladium-catalyzed cross-coupling polymerization: A new access to cross-conjugated polymers with modifiable structure and tunable optical/conductive properties. *Macromolecules* **2018**, *51*, 9662–9668. [CrossRef]

64. Amna, B.; Ateş, A.; Ozturk, T. Pd/Cu-catalyzed sonogashira cross-coupling polycondensation: A promising approach for synthesizing conjugated polymers with useful applications. *Eur. Polym. J.* **2023**, *196*, 112275. [CrossRef]

65. Howe, D.H.; McDaniel, R.M.; Magenau, A.J.D. From click chemistry to cross-coupling: Designer polymers from one efficient reaction. *Macromolecules* **2017**, *50*, 8010–8018. [CrossRef]

66. Pouliot, J.-R.; Grenier, F.; Blaskovits, J.T.; Beaupré, S.; Leclerc, M. Direct (hetero)arylation polymerization: Simplicity for conjugated polymer synthesis. *Chem. Rev.* **2016**, *116*, 14225–14274. [CrossRef]

67. Bura, T.; Blaskovits, J.T.; Leclerc, M. Direct (hetero)arylation polymerization: Trends and perspectives. *J. Am. Chem. Soc.* **2016**, *138*, 10056–10071. [CrossRef]

68. Yang, Z.-K.; Xu, N.-X.; Takita, R.; Muranaka, A.; Wang, C.; Uchiyama, M. Cross-coupling polycondensation via C–O or C–N bond cleavage. *Nat. Commun.* **2018**, *9*, 1587. [CrossRef] [PubMed]

69. Xu, S.; Kim, E.H.; Wei, A.; Negishi, E.-i. Pd- and Ni-catalyzed cross-coupling reactions in the synthesis of organic electronic materials. *Sci. Technol. Adv. Mater.* **2014**, *15*, 044201. [CrossRef] [PubMed]

70. Schroot, R.; Schubert, U.S.; Jäger, M. Poly(n-alkyl-3,6-carbazole)s via Kumada catalyst transfer polymerization: Impact of metal–halogen exchange. *Macromolecules* **2016**, *49*, 8801–8811. [CrossRef]

71. Cheng, S.; Ye, S.; Apte, C.N.; Yudin, A.K.; Seferos, D.S. Improving the Kumada catalyst transfer polymerization with water-scavenging grignard reagents. *ACS Macro Lett.* **2021**, *10*, 697–701. [CrossRef] [PubMed]

72. Hardeman, T.; Koeckelberghs, G. Synthesis of conjugated copolymers by combining different coupling reactions. *Polym. Chem.* **2017**, *8*, 3999–4004. [CrossRef]

73. Stefan, M.C.; Bhatt, M.P.; Sista, P.; Magurudeniya, H.D. Grignard metathesis (GRIM) polymerization for the synthesis of conjugated block copolymers containing regioregular poly(3-hexylthiophene). *Polym. Chem.* **2012**, *3*, 1693–1701. [CrossRef]

74. Wu, J.; Lan, Z.; Lin, J.; Huang, M.; Huang, Y.; Fan, L.; Luo, G.; Lin, Y.; Xie, Y.; Wei, Y. Counter electrodes in dye-sensitized solar cells. *Chem. Soc. Rev.* **2017**, *46*, 5975–6023. [CrossRef] [PubMed]

75. Wang, H.; Feng, Q.; Gong, F.; Li, Y.; Zhou, G.; Wang, Z.-S. In situ growth of oriented polyaniline nanowires array for efficient cathode of Co(III)/Co(II) mediated dye-sensitized solar cell. *J. Mater. Chem. A* **2013**, *1*, 97–104. [CrossRef]

76. Lee, J.H.; Jang, Y.J.; Kim, D.W.; Cheruku, R.; Thogiti, S.; Ahn, K.-S.; Kim, J.H. Application of polypyrrole/sodium dodecyl sulfate/carbon nanotube counter electrode for solid-state dye-sensitized solar cells and dye-sensitized solar cells. *Chem. Pap.* **2019**, *73*, 2749–2755. [CrossRef]

77. Chen, G.-F.; Su, Y.-Z.; Kuang, P.-Y.; Liu, Z.-Q.; Chen, D.-Y.; Wu, X.; Li, N.; Qiao, S.-Z. Polypyrrole Shell@3D-Ni metal core structured electrodes for high-performance supercapacitors. *Chem.-A Eur. J.* **2015**, *21*, 4614–4621. [CrossRef]

78. Hwang, D.K.; Song, D.; Jeon, S.S.; Han, T.H.; Kang, Y.S.; Im, S.S. Ultrathin polypyrrole nanosheets doped with HCl as counter electrodes in dye-sensitized solar cells. *J. Mater. Chem. A* **2014**, *2*, 859–865. [CrossRef]

79. Torabi, N.; Behjat, A.; Jafari, F. Dye-sensitized solar cells based on porous conjugated polymer counter electrodes. *Thin Solid Films* **2014**, *573*, 112–116. [CrossRef]

80. Bora, C.; Sarkar, C.; Mohan, K.J.; Dolui, S. Polythiophene/graphene composite as a highly efficient platinum-free counter electrode in dye-sensitized solar cells. *Electrochim. Acta* **2015**, *157*, 225–231. [CrossRef]

81. Zhang, R.; Li, Z.; Xu, J.; Xia, J. Synthesis and application of poly(bis-3,4-ethylenedioxythiophene methine)s as novel counter electrodes in dye-sensitized solar cells. *Sol. Energy* **2018**, *173*, 1189–1196. [CrossRef]

82. Naresh, V.; Elias, L.; Martha, S.K. Poly(3,4-ethylenedioxythiophene) coated lead negative plates for hybrid energy storage systems. *Electrochim. Acta* **2019**, *301*, 183–191. [CrossRef]

83. Zhang, J.; Long, H.; Miralles, S.G.; Bisquert, J.; Fabregat-Santiago, F.; Zhang, M. The combination of a polymer–carbon composite electrode with a high-absorptivity ruthenium dye achieves an efficient dye-sensitized solar cell based on a thiolate–disulfide redox couple. *Phys. Chem. Chem. Phys.* **2012**, *14*, 7131–7136. [CrossRef]

84. Chamatam Kasi Reddy, A.; Neeraja, V.; Meenakshamma, A.; Gurulakshmi, M.; Gurubhasker, M.; Raghavender, M.; Pedda Venkata Subbaiah, Y. Efficient counter electrode of MoS_2-GO/PEDOT:PSS for platinum-free, high performance dye sensitized solar cells. *ChemistrySelect* **2024**, *9*, e202305200. [CrossRef]

85. Vlachopoulos, N.; Grätzel, M.; Hagfeldt, A. Solid-state dye-sensitized solar cells using polymeric hole conductors. *RSC Adv.* **2021**, *11*, 39570–39581. [CrossRef] [PubMed]

86. Sangwan, B.; Kumar, S.; Singh, A.; Pandey, S.P.; Singh, P.K.; Singh, R.C.; Tomar, R. Modified poly(vinyl alcohol) based polymer electrolyte for dye sensitized solar cells (DSSCs). *Macromol. Symp.* **2023**, *407*, 2100462. [CrossRef]

87. Raut, P.; Kishnani, V.; Mondal, K.; Gupta, A.; Jana, S.C. A review on gel polymer electrolytes for dye-sensitized solar cells. *Micromachines* **2022**, *13*, 680. [CrossRef]

88. Chowdhury, F.I.; Buraidah, M.H.; Arof, A.K.; Mellander, B.E.; Noor, I.M. Impact of tetrabutylammonium, iodide and triiodide ions conductivity in polyacrylonitrile based electrolyte on DSSC performance. *Sol. Energy* **2020**, *196*, 379–388. [CrossRef]

89. Manikandan, K.; Yelilarasi, A.; Saravanakumar, S.; Althomali, R.H.; Khan, A.; Abualnaja, K.M.; Alhashmialameer, D.; Hussein, M. The effect of plasticizers on the polypyrrole-poly(vinyl alcohol)-based conducting polymer electrolyte and its application in semi-transparent dye-sensitized solar cells. *Membranes* **2021**, *11*, 791. [CrossRef]

90. Tarannum, N.; Varishetty, M.M. Synthesis of organic sulfobetaine-based polymer gel electrolyte for dye-sensitized solar cell application. *Polym. Adv. Technol.* **2017**, *28*, 1504–1509. [CrossRef]

91. Fang, Z.; Eshbaugh, A.A.; Schanze, K.S. Low-bandgap donor−acceptor conjugated polymer sensitizers for dye-sensitized solar cells. *J. Am. Chem. Soc.* **2011**, *133*, 3063–3069. [CrossRef] [PubMed]

92. Liu, X.; Zhu, R.; Zhang, Y.; Liu, B.; Ramakrishna, S. Anionic benzothiadiazole containing polyfluorene and oligofluorene as organic sensitizers for dye-sensitized solar cells. *Chem. Commun.* **2008**, *32*, 3789–3791. [CrossRef] [PubMed]

93. Giri, D.; Raut, S.K.; Patra, S.K. Diketopyrrolopyrrole/perylene-diimide and thiophene based D-π-A low bandgap polymer sensitizers for application in dye sensitized solar cells. *Dyes Pigm.* **2020**, *174*, 108032. [CrossRef]

94. Kim, Y.-G.; Walker, J.; Samuelson, L.A.; Kumar, J. Efficient light harvesting polymers for nanocrystalline TiO_2 photovoltaic cells. *Nano Lett.* **2003**, *3*, 523–525. [CrossRef]

95. Senadeera, G.K.R.; Kitamura, T.; Wada, Y.; Yanagida, S. Photosensitization of nanocrystalline TiO_2 films by a polymer with two carboxylic groups, poly (3-thiophenemalonic acid). *Sol. Energy Mater. Sol. Cells* **2005**, *88*, 315–322. [CrossRef]

96. Senadeera, G.K.R.; Nakamura, K.; Kitamura, T.; Wada, Y.; Yanagida, S. Fabrication of highly efficient polythiophene-sensitized metal oxide photovoltaic cells. *Appl. Phys. Lett.* **2003**, *83*, 5470–5472. [CrossRef]

97. Ohshita, J.; Matsukawa, J.; Hara, M.; Kunai, A.; Kajiwara, S.; Ooyama, Y.; Harima, Y.; Kakimoto, M. Attachment of disilanylene–oligothienylene polymers on TiO_2 surface by photochemical cleavage of the Si–Si bonds. *Chem. Lett.* **2008**, *37*, 316–317. [CrossRef]

98. Mwaura, J.K.; Zhao, X.; Jiang, H.; Schanze, K.S.; Reynolds, J.R. Spectral broadening in nanocrystalline TiO_2 solar cells based on poly(p-phenylene ethynylene) and polythiophene sensitizers. *Chem. Mater.* **2006**, *18*, 6109–6111. [CrossRef]

99. Marques, A.S.; Szostak, R.; Marchezi, P.E.; Nogueira, A.F. Perovskite solar cells based on polyaniline derivatives as hole transport materials. *J. Phys. Energy* **2019**, *1*, 015004. [CrossRef]

100. Jha, P.; Koiry, S.P.; Sridevi, C.; Gupta, D.; Putta, V.; Lenka, R.K.; Chauhan, A.K. Solution processable polypyrrole nanotubes as an alternative hole transporting material in perovskite solar cells. *Mater. Today Commun.* **2023**, *35*, 105994. [CrossRef]

101. Kegelmann, L.; Tockhorn, P.; Wolff, C.M.; Márquez, J.A.; Caicedo-Dávila, S.; Korte, L.; Unold, T.; Lövenich, W.; Neher, D.; Rech, B.; et al. Mixtures of dopant-free Spiro-OMeTAD and water-free PEDOT as a passivating hole contact in perovskite solar cells. *ACS Appl. Mater. Interfaces* **2019**, *11*, 9172–9181. [CrossRef]

102. Lim, K.-G.; Ahn, S.; Kim, H.; Choi, M.-R.; Huh, D.H.; Lee, T.-W. Self-doped conducting polymer as a hole-extraction layer in organic–inorganic hybrid perovskite solar cells. *Adv. Mater. Interfaces* **2016**, *3*, 1500678. [CrossRef]

103. Rai, N.; Reddy, S.S.; Scully, A.D.; Weerarathna, K.L.J.; Bach, U.; Simonov, A.N. Ester-functionalized polythiophene interlayers for enhanced performance and stability of perovskite solar cells. *Adv. Mater. Technol.* **2024**, *9*, 2301539. [CrossRef]

104. Gatti, T.; Casaluci, S.; Prato, M.; Salerno, M.; Di Stasio, F.; Ansaldo, A.; Menna, E.; Di Carlo, A.; Bonaccorso, F. Boosting perovskite solar cells performance and stability through doping a poly-3(hexylthiophene) hole transporting material with organic functionalized carbon nanostructures. *Adv. Funct. Mater.* **2016**, *26*, 7443–7453. [CrossRef]

105. Nia, N.Y.; Matteocci, F.; Cina, L.; Di Carlo, A. High-efficiency perovskite solar cell based on poly(3-hexylthiophene): Influence of molecular weight and mesoscopic scaffold layer. *ChemSusChem* **2017**, *10*, 3854–3860. [CrossRef] [PubMed]

106. Ren, W.; Liu, Y.; Wu, Y.; Sun, Q.; Cui, Y.; Hao, Y. Interface modification of an electron transport layer using europium acetate for enhancing the performance of P3HT-based inorganic perovskite solar cells. *Phys. Chem. Chem. Phys.* **2021**, *23*, 23818–23826. [CrossRef]

107. Duan, C.; Tang, A.; Guo, Q.; Zhang, W.; Yang, L.; Ding, Y.; Dai, Z.; Zhou, E. DTBDT-based polymer hole transport materials for low voltage loss CsPbI$_2$Br perovskite solar cells. *Adv. Funct. Mater.* **2024**, *34*, 2313462. [CrossRef]

108. Zhang, Z.; Fu, J.; Chen, Q.; Zhang, J.; Huang, Z.; Cao, J.; Ji, W.; Zhang, L.; Wang, A.; Zhou, Y.; et al. Dopant-free polymer hole transport materials for highly stable and efficient CsPbI$_3$ perovskite solar cells. *Small* **2023**, *19*, 2206952. [CrossRef] [PubMed]

109. Zhao, M.; Zong, X.; Chen, Y.; Liu, P.; Xiong, Y.; Zhang, W.; He, J.; Wang, Z.; Xue, S. Flexible backbone-assisted green-solvent processable polymer hole transport material in perovskite solar cells. *ACS Sustain. Chem. Eng.* **2024**, *12*, 1941–1950. [CrossRef]

110. Fu, Q.; Liu, H.; Gao, Y.; Cao, X.; Li, Y.; Yang, Y.; Wang, J.; Chen, Y.; Yao, Z.; Liu, Y. Tunable molecular packing of dopant-free hole-transport polymers for perovskite solar cells. *ACS Energy Lett.* **2023**, *8*, 2878–2885. [CrossRef]

111. Wang, W.; Yuan, J.; Shi, G.; Zhu, X.; Shi, S.; Liu, Z.; Han, L.; Wang, H.-Q.; Ma, W. Inverted planar heterojunction perovskite solar cells employing polymer as the electron conductor. *ACS Appl. Mater. Interfaces* **2015**, *7*, 3994–3999. [CrossRef] [PubMed]

112. Guo, Y.; Sato, W.; Inoue, K.; Zhang, W.; Yu, G.; Nakamura, E. n-Type doping for efficient polymeric electron-transporting layers in perovskite solar cells. *J. Mater. Chem. A* **2016**, *4*, 18852–18856. [CrossRef]

113. Guo, Q.; Xu, Y.; Xiao, B.; Zhang, B.; Zhou, E.; Wang, F.; Bai, Y.; Hayat, T.; Alsaedi, A.; Tan, Z. Effect of energy alignment, electron mobility, and film morphology of perylene diimide based polymers as electron transport layer on the performance of perovskite solar cells. *ACS Appl. Mater. Interfaces* **2017**, *9*, 10983–10991. [CrossRef] [PubMed]

114. Sun, C.; Wu, Z.; Yip, H.-L.; Zhang, H.; Jiang, X.-F.; Xue, Q.; Hu, Z.; Hu, Z.; Shen, Y.; Wang, M.; et al. Amino-functionalized conjugated polymer as an efficient electron transport layer for high-performance planar-heterojunction perovskite solar cells. *Adv. Energy Mater.* **2016**, *6*, 1501534. [CrossRef]

115. Hoang Huy, V.P.; Bark, C.-W. Polymer-doped SnO$_2$ as an electron transport layer for highly efficient and stable perovskite solar cells. *Polymers* **2024**, *16*, 199. [CrossRef]

116. Kranthiraja, K.; He, W.; Yu, H.-W.; Feng, Z.; Nozaki, N.; Matsumoto, H.; Yu, M.-H.; Li, Y.; Manzhos, S.; Andersson, M.R.; et al. Diketopyrrolopyrrole-dioxo-benzodithiophene-based multifunctional conjugated polymers for organic field-effect transistors and perovskite solar cells. *Solar RRL* **2024**, *8*, 2400185. [CrossRef]

117. Anrango-Camacho, C.; Pavón-Ipiales, K.; Frontana-Uribe, B.A.; Palma-Cando, A. Recent advances in hole-transporting layers for organic solar cells. *Nanomaterials* **2022**, *12*, 443. [CrossRef] [PubMed]

118. Cai, W.; Musumeci, C.; Ajjan, F.N.; Bao, Q.; Ma, Z.; Tang, Z.; Inganäs, O. Self-doped conjugated polyelectrolyte with tuneable work function for effective hole transport in polymer solar cells. *J. Mater. Chem. A* **2016**, *4*, 15670–15675. [CrossRef]

119. Hamui, L.; Sánchez-Vergara, M.E.; Corona-Sánchez, R.; Jiménez-Sandoval, O.; Álvarez-Toledano, C. Innovative incorporation of poly(3,4-ethylenedioxythiophene)-poly(styrenesulfonate) as hole carrier transport layer and as anode for organic solar cells performance improvement. *Polymers* **2020**, *12*, 2808. [CrossRef] [PubMed]

120. Pietsch, M.; Bashouti, M.Y.; Christiansen, S. The role of hole transport in hybrid inorganic/organic silicon/poly(3,4-ethylenedioxy-thiophene):Poly(styrenesulfonate) heterojunction solar cells. *J. Phys. Chem. C* **2013**, *117*, 9049–9055. [CrossRef]

121. Li, Y.; Hong, N. An efficient hole transport material based on PEDOT dispersed with lignosulfonate: Preparation, characterization and performance in polymer solar cells. *J. Mater. Chem. A* **2015**, *3*, 21537–21544. [CrossRef]

122. Xu, J.; Heumüller, T.; Le Corre, V.M.; Barabash, A.; Félix, R.; Frisch, J.; Bär, M.; Brabec, C.J. A polymer bilayer hole transporting layer architecture for high-efficiency and stable organic solar cells. *Joule* **2024**, *8*, 2570–2584. [CrossRef]

123. Jiang, Y.; Dong, X.; Sun, L.; Liu, T.; Qin, F.; Xie, C.; Jiang, P.; Hu, L.; Lu, X.; Zhou, X.; et al. An alcohol-dispersed conducting polymer complex for fully printable organic solar cells with improved stability. *Nat. Energy* **2022**, *7*, 352–359. [CrossRef]

124. Moon, S.; Khadtare, S.; Wong, M.; Han, S.-H.; Bazan, G.C.; Choi, H. Hole transport layer based on conjugated polyelectrolytes for polymer solar cells. *J. Colloid Interface Sci.* **2018**, *518*, 21–26. [CrossRef]

125. Zhou, H.; Zhang, Y.; Mai, C.-K.; Collins, S.D.; Nguyen, T.-Q.; Bazan, G.C.; Heeger, A.J. Conductive Conjugated Polyelectrolyte as Hole-Transporting Layer for Organic Bulk Heterojunction Solar Cells. *Adv. Mater.* **2014**, *26*, 780–785. [CrossRef] [PubMed]

126. Xu, H.; Fu, X.; Cheng, X.; Huang, L.; Zhou, D.; Chen, L.; Chen, Y. Highly and homogeneously conductive conjugated polyelectrolyte hole transport layers for efficient organic solar cells. *J. Mater. Chem. A* **2017**, *5*, 14689–14696. [CrossRef]

127. Liu, S.; You, P.; Li, J.; Li, J.; Lee, C.-S.; Ong, B.S.; Surya, C.; Yan, F. Enhanced efficiency of polymer solar cells by adding a high-mobility conjugated polymer. *Energy Environ. Sci.* **2015**, *8*, 1463–1470. [CrossRef]

128. Al-Azzawi, A.G.S.; Aziz, S.B.; Dannoun, E.M.A.; Iraqi, A.; Nofal, M.M.; Murad, A.R.; Hussein, A.M. A mini review on the development of conjugated polymers: Steps towards the commercialization of organic solar cells. *Polymers* **2023**, *15*, 164. [CrossRef] [PubMed]

129. Tetreault, A.R.; Dang, M.-T.; Bender, T.P. PTB7 and PTB7-Th as universal polymers to evaluate materials development aspects of organic solar cells including interfacial layers, new fullerenes, and non-fullerene electron acceptors. *Synth. Met.* **2022**, *287*, 117088. [CrossRef]

130. Ohori, Y.; Fujii, S.; Kataura, H.; Nishioka, Y. Improvement of bulk heterojunction organic solar cells based on PTB7:PC$_{61}$BM with small amounts of P3HT. *Jpn. J. Appl. Phys.* **2015**, *54*, 04DK09. [CrossRef]

131. Shaban, M.; Benghanem, M.; Almohammedi, A.; Rabia, M. Optimization of the active layer P3HT:PCBM for organic solar cell. *Coatings* **2021**, *11*, 863. [CrossRef]

132. Tang, Y.; Liu, L.; Deng, J.; Sun, P.; Yan, D.; Peng, W.; Huang, X.; Xiao, M.; Tao, Q.; Yu, D. Incorporating a weak acceptor unit into PTB7-Th to tune the open circuit voltage for non-fullerene polymer solar cells. *Tetrahedron* **2023**, *131*, 133214. [CrossRef]

133. Ko, S.-J.; Walker, B.; Nguyen, T.L.; Choi, H.; Seifter, J.; Uddin, M.A.; Kim, T.; Kim, S.; Heo, J.; Kim, G.-H.; et al. Photocurrent extraction efficiency near unity in a thick polymer bulk heterojunction. *Adv. Funct. Mater.* **2016**, *26*, 3324–3330. [CrossRef]

134. Lin, Q.; Stoltzfus, D.M.; Armin, A.; Burn, P.L.; Meredith, P. An hydrophilic anode interlayer for solution processed organohalide perovskite solar cells. *Adv. Mater. Interfaces* **2016**, *3*, 1500420. [CrossRef]

135. Freitag, M.; Teuscher, J.; Saygili, Y.; Zhang, X.; Giordano, F.; Liska, P.; Hua, J.; Zakeeruddin, S.M.; Moser, J.-E.; Grätzel, M.; et al. Dye-sensitized solar cells for efficient power generation under ambient lighting. *Nat. Photonics* **2017**, *11*, 372–378. [CrossRef]

136. Cao, Y.; Liu, Y.; Zakeeruddin, S.M.; Hagfeldt, A.; Grätzel, M. Direct contact of selective charge extraction layers enables high-efficiency molecular photovoltaics. *Joule* **2018**, *2*, 1108–1117. [CrossRef]

137. Venkatesan, S.; Lin, W.-H.; Hsu, T.-H.; Teng, H.; Lee, Y.-L. Indoor dye-sensitized solar cells with efficiencies surpassing 26% using polymeric counter electrodes. *ACS Sustain. Chem. Eng.* **2022**, *10*, 2473–2483. [CrossRef]

138. Guo, Z.; Jena, A.K.; Takei, I.; Ikegami, M.; Ishii, A.; Numata, Y.; Shibayama, N.; Miyasaka, T. Dopant-free polymer HTM-based CsPbI$_2$Br solar cells with efficiency over 17% in sunlight and 34% in indoor light. *Adv. Funct. Mater.* **2021**, *31*, 2103614. [CrossRef]

139. Ding, Z.; Zhao, R.; Yu, Y.; Liu, J. All-polymer indoor photovoltaics with high open-circuit voltage. *J. Mater. Chem. A* **2019**, *7*, 26533–26539. [CrossRef]

140. Jiang, F.; Liu, T.; Zeng, S.; Zhao, Q.; Min, X.; Li, Z.; Tong, J.; Meng, W.; Xiong, S.; Zhou, Y. Metal electrode–free perovskite solar cells with transfer-laminated conducting polymer electrode. *Opt. Express* **2015**, *23*, A83–A91. [CrossRef]

141. Jiang, Y.; Luo, B.; Jiang, F.; Jiang, F.; Fuentes-Hernandez, C.; Liu, T.; Mao, L.; Xiong, S.; Li, Z.; Wang, T.; et al. Efficient Colorful Perovskite Solar Cells Using a Top Polymer Electrode Simultaneously as Spectrally Selective Antireflection Coating. *Nano Lett.* **2016**, *16*, 7829–7835. [CrossRef] [PubMed]

142. Jiang, Y.; Liu, T.; Zhou, Y. Recent advances of synthesis, properties, film fabrication methods, modifications of poly(3,4-ethylenedioxythiophene), and applications in solution-processed photovoltaics. *Adv. Funct. Mater.* **2020**, *30*, 2006213. [CrossRef]

143. Kim, Y.; Ryu, T.I.; Ok, K.-H.; Kwak, M.-G.; Park, S.; Park, N.-G.; Han, C.J.; Kim, B.S.; Ko, M.J.; Son, H.J.; et al. Inverted layer-by-layer fabrication of an ultraflexible and transparent Ag nanowire/conductive polymer composite electrode for use in high-performance organic solar cells. *Adv. Funct. Mater.* **2015**, *25*, 4580–4589. [CrossRef]

144. Xu, Y.; Lin, Z.; Wei, W.; Hao, Y.; Liu, S.; Ouyang, J.; Chang, J. Recent progress of electrode materials for flexible perovskite solar cells. *Nano-Micro Lett.* **2022**, *14*, 117. [CrossRef]

145. Bu, L.; Liu, Z.; Zhang, M.; Li, W.; Zhu, A.; Cai, F.; Zhao, Z.; Zhou, Y. Semitransparent fully air processed perovskite solar cells. *ACS Appl. Mater. Interfaces* **2015**, *7*, 17776–17781. [CrossRef]

146. Aivali, S.; Beaumont, C.; Leclerc, M. Conducting polymers: Towards printable transparent electrodes. *Prog. Polym. Sci.* **2024**, *148*, 101766. [CrossRef]

147. Ponder, J.F., Jr.; Österholm, A.M.; Reynolds, J.R. Conjugated polyelectrolytes as water processable precursors to aqueous compatible redox active polymers for diverse applications: Electrochromism, charge storage, and biocompatible organic electronics. *Chem. Mater.* **2017**, *29*, 4385–4392. [CrossRef]

148. Ke, Z.; Abtahi, A.; Hwang, J.; Chen, K.; Chaudhary, J.; Song, I.; Perera, K.; You, L.; Baustert, K.N.; Graham, K.R.; et al. Highly conductive and solution-processable n-doped transparent organic conductor. *J. Am. Chem. Soc.* **2023**, *145*, 3706–3715. [CrossRef]

149. Chen, X.; Liu, J.; Qian, K.; Wang, J. Ternary composites of Ni–polyaniline–graphene as counter electrodes for dye-sensitized solar cells. *RSC Adv.* **2018**, *8*, 10948–10953. [CrossRef] [PubMed]

150. Wu, K.; Zhao, Q.; Chen, L.; Ruan, B.; Wu, M. Impact of electrocatalytic activities of doping surfactants on polyaniline as Pt-free counter electrode in DSSCs. *Int. J. Electrochem. Sci.* **2018**, *13*, 4868–4875. [CrossRef]

151. Lee, K.-M.; Chen, P.-Y.; Hsu, C.-Y.; Huang, J.-H.; Ho, W.-H.; Chen, H.-C.; Ho, K.-C. A high-performance counter electrode based on poly(3,4-alkylenedioxythiophene) for dye-sensitized solar cells. *J. Power Sources* **2009**, *188*, 313–318. [CrossRef]

152. Duan, C.; Willems, R.E.M.; van Franeker, J.J.; Bruijnaers, B.J.; Wienk, M.M.; Janssen, R.A.J. Effect of side chain length on the charge transport, morphology, and photovoltaic performance of conjugated polymers in bulk heterojunction solar cells. *J. Mater. Chem. A* **2016**, *4*, 1855–1866. [CrossRef]

153. Chen, L.; Liu, W.; Yan, Y.; Su, X.; Xiao, S.; Lu, X.; Uher, C.; Tang, X. Fine-tuning the solid-state ordering and thermoelectric performance of regioregular P3HT analogues by sequential oxygen-substitution of carbon atoms along the alkyl side chains. *J. Mater. Chem. C* **2019**, *7*, 2333–2344. [CrossRef]

154. Li, Y.; Sha, M.; Huang, S. A review on transparent electrodes for flexible organic solar cells. *Coatings* **2024**, *14*, 1031. [CrossRef]